Advances and challenges in tuning the reversibility & cyclability of room temperature sodium–sulfur and potassium–sulfur batteries with catalytic materials

Anupriya K. Haridas [a], Chun Huang [b, c, *]

[a] Department of Engineering, King's College London, London, WC2R 2LS, United Kingdom
[b] Department of Materials, Imperial College London, London, SW7 2AZ, United Kingdom
[c] The Faraday Institution, Quad One, Becquerel Ave, Harwell Campus, Didcot, OX11 0RA, United Kingdom

ARTICLE INFO

ABSTRACT

The high theoretical energy density of room temperature sodium-sulfur and potassium-sulfur batteries (Na–S; 1274 Wh/kg, K–S; 914 Wh/kg; based on the mass of sulfur) due to the multi-electron transfer associated with the unique conversion chemistry of S and the natural abundance of Na, K, and S raw materials make them ideal candidates for large-scale energy storage applications beyond Li batteries. However, achieving good reversibility, cyclability, and active material utilization in Na–S and K–S batteries demands alleviation of the complex polysulfide dissolution and the shuttle phenomena during cycling. Rational employment of catalytic materials is beneficial to address these issues by facilitating effective polysulfide transformation and thereby accelerating the sluggish reaction kinetics. This review focuses on the roles and evolution of catalytic materials in polysulfide adsorption, catalytic conversion, and redox mediation in facilitating high-performing Na–S and K–S batteries. Specifically, the advances in tuning the reversibility and cyclability of Na-S and K–S batteries strategically with catalytic material-incorporated S-host cathodes, separators, and interlayers and the interaction of various catalytic materials with the polysulfide species are discussed in the light of advanced characterization techniques. Lastly, the challenges and the plausible strategies for future research are elucidated.

1. Introduction

Climate change and the fast depletion of natural resources have endorsed the idea of exploring renewable energy resources, promoting net-zero carbon emissions. Such efforts have popularized the use of electric vehicles and large-scale grid storage systems, crowning energy storage technology as the cutting-edge research field of the decade. Specifically, energy storage systems (EES) that offer high energy density and extended cycle life are of substantial interest in integrating renewable energy resources into the electrical grid. Given that the energy requirements in EEEs are projected to reach 167 GWh by 2030, owing to the wide range of these prospective applications, using conventional lithium-ion batteries (LIBs) only which have substantial raw materials and production costs (~500 USD kW/h) is not a feasible solution [1,2]. On the contrary, next-generation batteries like Na/K-ion batteries and metal-sulfur (M–S) batteries are comparatively inexpensive and eco-friendly and offer on par or even better energy storage properties compared to commercialized LIBs [3,4]. Among them, M–S batteries that utilize the multi-electron transfer reactions are of great interest, on account of the achievable high gravimetric capacity (1675 mAh/g) associated with sulfur and have emerged as potential alternatives for stationary and large-scale energy storage applications [4].

Benefitting from the reduced cost of production owing to the abundance of raw materials (Na and K as illustrated in Fig. 1a) and the projected high theoretical energy densities, advanced M-S-based battery systems like room temperature sodium-sulfur (Na–S) and potassium sulfur (K–S) batteries have been on global research focus recently [5–7]. Though Na–S batteries have been researched since the 1980s, the global research interest in Na–S batteries peaked in the past decade. With the technological advances and the success of their predecessor, lithium-sulfur (Li–S) batteries, many research problems in Na–S battery research are

* Corresponding author.
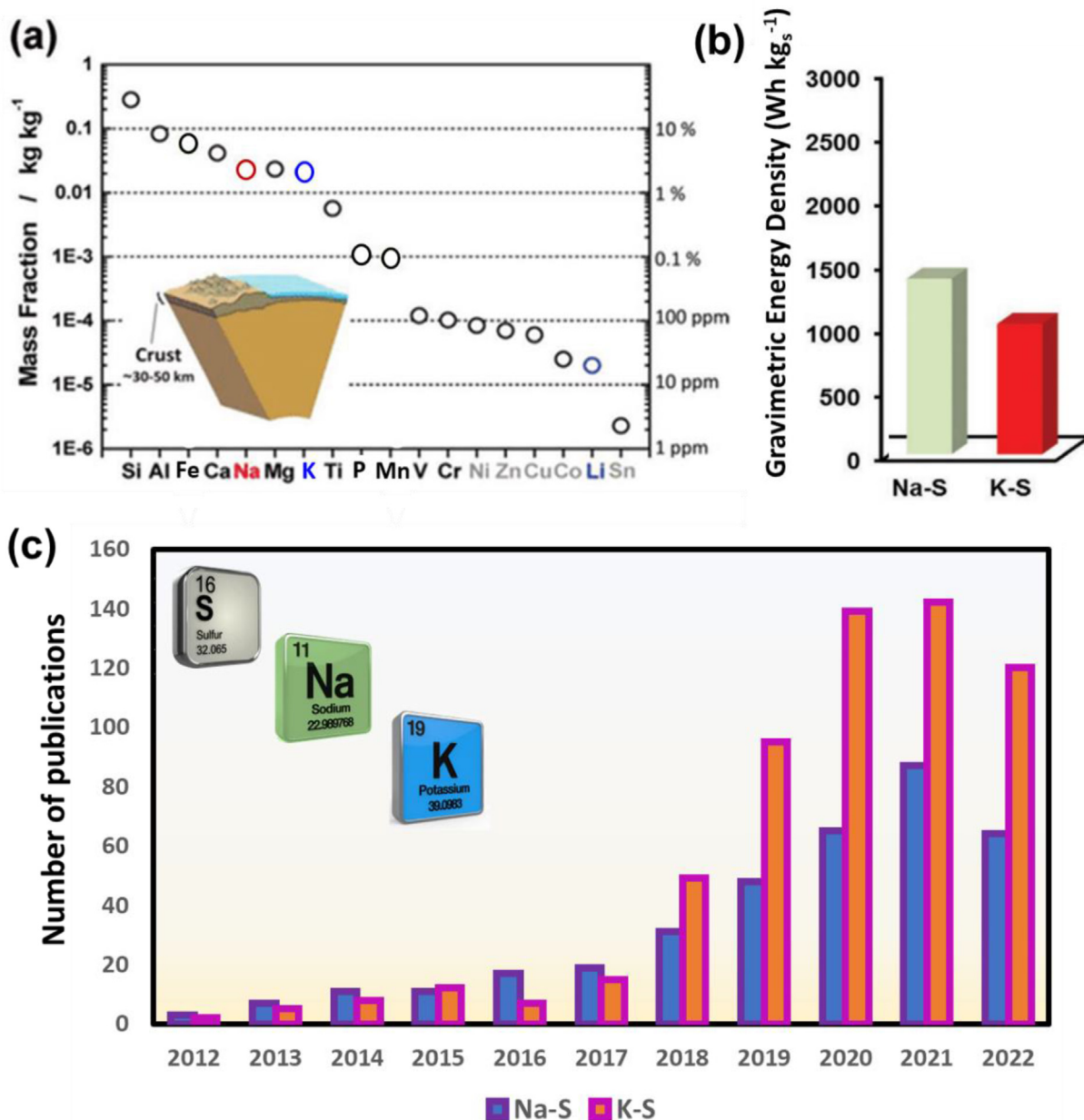E-mail address: a.huang@imperial.ac.uk (C. Huang).

Fig. 1. Comparison of a) geographical abundance of Na and K. Reprinted (adapted) with permission from Ref. [7]. Copyright 2014 American Chemical Society. and b) energy density. Reprinted (adapted) with permission from Ref. [6]. Copyright 2020 John Wiley and Sons. c) recent trend of publications in Na−S and K−S batteries (Source: *Scopus*, retrieved from the search of "room-temperature sodium-sulfur batteries" and "potassium sulfur batteries," on October 7, 2022).

being addressed by drawing parallels from them. However, the differences in the stability of polysulfide intermediates and reaction pathways, along with the presence of a highly reactive anode, make Na−S and K−S battery chemistries more complex than Li−S batteries [8]. Despite these challenges, the steady rise in publications on Na−S and K−S batteries over the past decade (Fig. 1c) demonstrates the progressively growing global research interest in these advanced metal-sulfur battery systems because of their prospective applications.

Catalytic materials have been widely employed to boost redox-mediated processes and gas evolutions in chemical industries and to facilitate the development of cleaner energy technologies [9]. Recent ubiquitous applications of catalytic materials in areas that involve electrochemical reactions have transformed the field of energy conversion and storage [10,11]. Such electrocatalysts can aid

substantial acceleration of charge transfer on the interface of electrode and promote the reaction kinetics. It is interesting to note that, the concept of electrocatalysis has been applied to yield complete polysulfide transformations and accelerate the reaction kinetics in Li−S batteries, facilitating excellent electrochemical performances [12−14]. Following the trail, chemical adsorption strategies with electrocatalytic materials have also been extended to Na−S and K−S batteries very recently for catalytic polysulfide transformation and redox mediation [15,16]. However, the principles of engineering these materials and the reaction mechanisms involved are still not investigated and understood completely. Henceforth, it is critical to investigate the fundamentals of polysulfide redox transformations and the associated performance improvement in Na−S and K−S batteries under the influence of catalytic materials. Specifically, the determination of the active

2

centers of different catalysts, outlining the design principles for engineering the catalytic materials, and investigating their ability to tune the reversibility and cyclability of Na—S/K—S batteries would be highly desirable. This review focuses on the advances and impact of employing various catalytic materials in Na—S and K—S batteries in the light of advanced characterizations and provides insights and future directions for engineering advanced catalytic materials tailored for the performance improvement of these advanced M—S battery systems.

2. Na—S *vs.* K—S batteries: fundamentals & electrochemistry

The fundamental electrochemical reactions in Na—S and K—S batteries are discussed in this section. The configuration of Na—S and K—S batteries is analogous to the Li—S batteries. Typically, Na—S/K—S cells consist of an S cathode and a Na/K metal anode, along with a separator soaked in a non-aqueous electrolyte, as shown in Fig. 2a. The electrochemical characteristics of Na—S and K—S battery systems are compared in Table 1. The intermediate polysulfide species and the number of electrons transferred in Na—S and K—S batteries vary significantly because of the differences in the thermodynamic stability of intermediate NaPS and KPS species.

Na—S batteries work based on the electrochemical conversion reactions between Na^+ and S, resulting in a series of NaPS transformations. During discharge, the Na-ions from the Na anode migrate to the S cathode via the separator while the generated electrons pass through the external circuit towards the S cathode. This results in the reduction of S_8 to form sodium disulfide (Na_2S) at the end of discharge via formation of a series of sodium polysulfide (NaPS) species of varying chain lengths by the ring-opening of S_8 species.

During charging the process reverses forming S at the cathode, simultaneously replenishing the Na at the anode. However, the multi-step conversion reaction to form Na_2S via the formation of different intermediate polysulfides involves complex chemistries that lead to polysulfide shuttle mechanism and capacity degradation that calls for comprehensive research. Typically, the initial step of the conversion reaction begins with a solid-to-liquid transition due to the formation of high-order polysulfide Na_2S_8 in a liquid state [20]. Upon further discharge, Na_2S_8 is reduced to Na_2S_4 [20]. The following conversion reaction of Na_2S_4 to form low-order polysulfide (Na_2S_n, $1 \leq n \leq 4$) occurs via a liquid-to-solid state transition. The final discharge product is generated from the solid-solid transition from Na_2S_2 to Na_2S [20]. Among the various intermediate NaPS, the stable phases at RT are observed to be Na_2S_5, Na_2S_4, Na_2S_2, and Na_2S, and based on the polysulfide species formed at various stages, the number of electrons transferred varies directly impacting the specific capacity [21–23]. The polysulfide transformations and the associated number of electrons transferred in both Na—S and K—S batteries are illustrated in Fig. 2b and c, respectively [6,19].

The typical discharge profile of Na—S batteries with S_8 species and small sulfur molecules (S_2–S_4) or chemically bonded S species are provided in Fig. 3a and c, respectively. In the case of S_8 species, the high-voltage plateau region at 2.2 V corresponds to the conversion of S_8 to Na_2S_8 [22,24]. The sloping area from 2.2 to 1.65 V corresponds to the further reduction of Na_2S_8 to Na_2S_4. These intermediate species are soluble in ether electrolytes, though the lower-order polysulfides formed at lower voltages are solid species insoluble in electrolytes. The voltage plateau at 1.65 V corresponds to the liquid-solid transition between Na_2S_4 and Na_2S_3/Na_2S_2 [22]. The final discharge product Na_2S is formed at the voltage range from 1.65 to 1.2 V. The subsequent charge process involves the

oxidation of Na_2S to form Na_2S_4 and Na_2S_x, without the formation of Na_2S_2. Finally, S_8 is formed at the end of the charging process by a series of reduction reactions of the intermediate polysulfides. Nevertheless, the conversion reaction of small S molecules or chemically bonded S species and Na^+ occurs via a two-stage process, as shown in Fig. 3c [25]. The initial step corresponding to the voltage profile above 1.4 V leads to the formation of Na_2S_2, and the second step consists of the reduction of Na_2S_2 to Na_2S indicated by the plateau region below 1.4 V [25].

The charge/discharge process in K—S batteries also involves the reversible removal/replenishment of K metal at the anode and the oxidation/reduction reaction of S at the cathode. The discharge process of S_8 in K—S batteries is akin to that of Na—S batteries consisting of the formation of both the higher-order potassium polysulfides (KPS) like K_2S_n ($5 \leq n \leq 6$) in the liquid phase and insoluble lower-order polysulfides K_2S_n ($1 \leq n \leq 4$) [26,28]. Among the KPSs, K_2S_n (n = 1, 2, 3, 4, 5, and 6) are stable at RT [29,30]. Fig. 3b shows the discharge/charge profile of K—S batteries with an S_8 cathode. The phase transformation from S_8 to end discharge product K_2S is indicated by the sloping region between 2.25 and 1.65 V, while the plateau region from 1.6 to 1.2 V corresponds to the conversion of the K_2S_6 phase to K_2S_4 and K_2S_2 [28]. The final discharge product K_2S is formed as the reaction proceeds via the sloping region between 1.2 and 1 V [28]. It is to be noted that the voltage profile of chemically bonded S is significantly different as the redox reactions occur at a relatively lower potential (Fig. 3d). The region from 2 to 1 V indicates the formation of K_2S_3 and K_2S_2. Upon further reduction till 0.3 V, K_2S_3, K_2S_2, and K_2S phases coexist [27]. Additionally, the K_2S phase forms and coexists with K_2S_2 and K_2S_3 in the voltage range from 0.3 to 0.1 V. The main difference between the K—S system with Na—S batteries is the coexistence of K_2S_3 in the final discharge product owing to its higher thermodynamical stability in comparison with K_2S and is considered as a thermodynamic trap that limits the capacity of the system [27]. Thus, the disproportionation reaction forming K_2S_3 and K_2S leads to incomplete reduction and sluggish reaction kinetics that adversely affects the reversibility and cyclability of K—S batteries [31,32].

Though Na—S and K—S batteries offer similar S redox reaction pathways, there are significant differences in the intermediate polysulfides generated and the corresponding potentials. There has been evidence of irreversibility in Na—S and K—S batteries in the charging process. For e.g., in the Na—S system, Na_2S_x (x > 2) coexists with S due to the irreversible oxidation of the final discharge product Na_2S. At the same time, in K—S batteries, the incomplete oxidation of discharged products K_2S_3, K_2S_2, and K_2S results in the coexistence of K_2S_5 and K_2S_6 at a charged state [33]. Additionally, the formation of K_2S as the final discharge process significantly contributes to the irreversibility, resulting in the accumulation of K_2S in the following cycles [34]. The potentials at which the sodium and KPSs are generated also vary significantly (formation of Na_2S occurs at 1.65–1.2 V, while K_2S occurs at a lower voltage of 1.2–1 V.

3. Na—S & K—S batteries: concerns & challenges

Room temperature Na—S and K—S batteries face inherent challenges in achieving the theoretical capacity, energy density, and long-term cyclability unlike that of the Li—S system. The various challenges are described below.

a) *Non-conductive active material:* The intrinsic insulating nature of S ($\sim 5.13 \times 10^{-28}$ S/m) deteriorates the efficient transport of electrons within the cathode structure [35]. This leads to low S utilization, poor rate performance, and high
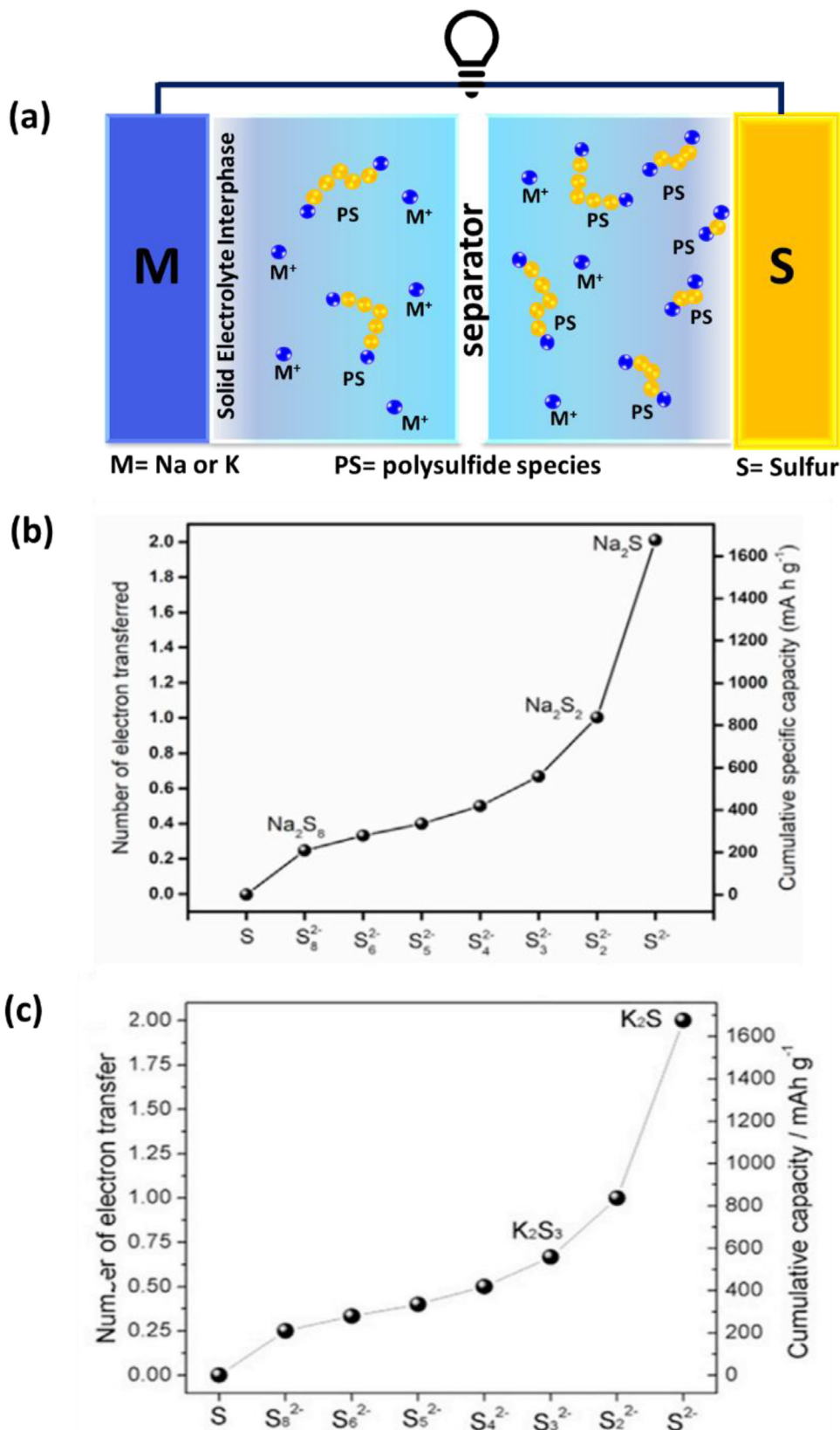
Fig. 2. a) Basic configuration of metal-sulfur batteries along with the number of electron transfers associated with Na−S and K−S batteries, polysulfide conversion and associated number of electrons transferred in b) Na−S Reprinted (adapted) with permission from Ref. [19]. Copyright 2022 Elsevier. and c) K−S batteries. Reprinted (adapted) with permission from Ref. [6]. Copyright 2020 John Wiley and Sons.

Table 1
Comparison of the characteristics of Na−S and K−S batteries [17,18].

Metal-Sulfur System	Na−S	K−S
Theoretical voltage [E^0, V]	1.85	1.88
Gravimetric energy density [Wh/kg]	1273	914
Volumetric energy density [Wh/L]	2363	1590
Electrochemical reaction	$2Na + 1/8S_8 \Longleftrightarrow Na_2S$	$2K + 1/8S_8 \Longleftrightarrow K_2S$
Volume expansion [ΔV, %]	171	309
Stable phases at RT	$Na_2S, Na_2S_2, Na_2S_4, Na_2S_5$	$K_2S, K_2S_2, K_2S_3, K_2S_4, K_2S_5, K_2S_6$

internal resistance in the cell. The accumulation of discharged products (Na_2S/K_2S) that are formed during electrochemical processes further builds up resistance in the cathode.

b) *Huge volume changes:* Volume expansion is a serious concern that severely affects the durability of Na−S and K−S batteries. The volume change in Na−S and K−S batteries is more prominent than in Li−S batteries due to the larger size of Na^+ and K^+ than Li^+. During the conversion process, the electrochemical reaction of S with Na^+/K^+ forms a series of high- and low-order polysulfides. The complete sodiation process forming the final discharge product Na_2S results in a volume change of ~171% [36]. Similarly, the formation of K_2S in K−S batteries induces a volume change of ~309% [37]. Such dramatic volume changes lead to the pulverization of cathodes and the loss of their structural integrity.

c) *Sluggish reaction kinetics:* The capacity generated from the conversion reaction between Na_2S_2/K_2S_2 and Na_2S/K_2S contributes to approximately two-thirds of the theoretical capacity of S. However, the reaction kinetics of the $Na_2S_4 \rightarrow Na_2S$ and $K_2S_3 \rightarrow K_2S$ conversions involve liquid-solid and solid-solid reactions respectively, which are inherently sluggish in nature. Moreover, the KPS intermediate K_2S_3 is thermodynamically stable compared with K_2S in K−S batteries, naturally favoring the formation of K_2S_3 than K_2S [31]. Overall, the slow reaction kinetics and incomplete reactions result in low active material utilization and irreversibility of reaction in both Na−S and K−S batteries.

d) *Polysulfide shuttle and loss of active material:* Polysulfide shuttle effect is a significant challenge in Na−S and K−S batteries, as it deteriorates cycle life and Coulombic efficiency (CE), promoting self-discharge in cells [38]. The effect is caused by the generation of long-chain polysulfides that are highly soluble in organic solvents, their subsequent migration toward the Na/K anode, and the reduction to form insoluble short-chain polysulfide species (Na_xS_n/K_xS_n). Additionally, the reduced polysulfides at the anode can diffuse back to the cathode and re-oxidize, causing self-discharge in cells and increasing the charge transfer resistance in cells tremendously.

e) *Highly reactive anode and unstable SEI:* Na−S and K−S batteries use metal Na and K as the anode, respectively, and this increases safety risk. Because side reactions take place between the anode and electrolyte, a non-uniform solid electrolyte interphase (SEI) layer is formed, which allows for uneven electroplating of Na^+/K^+ at the anode and results in the formation of Na/K dendritic growth [6,39]. Moreover, polysulfide species migrate toward the anode deposit on the anode surface, increasing the internal resistance of the cell. Additionally, the gradual formation of cracks on the surface of Na anode during the discharge process, along with needle-like structures of Na and non-uniform S deposits, also occur.

4. Significance and advances of catalytic materials for Na−S and K−S batteries

In Na−S and K−S batteries, the sluggish kinetics of NaPS/KPS redox reaction results in various soluble polysulfides, which shuttle between the cathode and anode, thus inducing anode corrosion and severe self-discharge. In the last few years, tremendous efforts have been devoted to addressing the above challenge and many strategies have been proposed incorporating materials or structures to entrap polysulfides. Physically blocking the migration of corresponding polysulfide species to the metallic anode is the most common and simplest method adopted to alleviate the shuttle phenomenon. Non-polar carbon materials with tunable porosity and nano architectures have been extensively developed and employed as S hosts and interlayers to block the migration of polysulfide species via physical confinement. However, this strategy has its drawbacks, including ineffective encapsulation and weak binding of polar polysulfide species with the non-polar substrates and is not always effective. Nevertheless, involving multi-electron redox reactions and a series of sophisticated phase transformations, an inherently slow polysulfide redox process cannot be accelerated effectively by mere adsorption from trapping materials. As a combination of chemical and physical adsorption strategies has been proposed to effectively mitigate polysulfide shuttling, the idea of employing electrocatalysts in Na−S and K−S batteries is highly desired to catalyze the polysulfide redox reactions and to accelerate the reduction of S species in Na−S and K−S batteries.

Catalysis in general is a process that enhances the rate of reaction without altering the overall change in standard Gibbs free energy of the reaction. Accordingly, catalytic materials or catalysts are the substances that facilitate catalysis i.e., improve the rate of a reaction, without being consumed during the reaction. Typically, energy conversion in an electrochemical reaction follows the Arrhenius equation, $k = Ae^{-Ea/RT}$, where k is the rate constant of the electrochemical reaction, A is the pre-exponential factor, E_a is the activation energy for the reaction to occur, R is the gas constant, and T is the associated temperature. Accordingly, the activation energy required for the reaction is inversely proportional to the rate of the electrochemical reaction. Thus, improving the rate of reaction can reduce the activation energy for the reaction, facilitating rapid and complete electrochemical processes and energy storage. The synergistic play of adsorption and catalysis offered by electrocatalytic materials in simultaneously enhancing the polysulfide aggregation and rate of polysulfide transformation of Li−S batteries resulting in effective utilization of active materials is noteworthy [40]. Unlike that of Na−S batteries, the exact final K_2S_n phase is not fully established. An incomplete reduction of higher order K_2S_n species is commonly reported which limits the capacity of the K−S system. For example, apart from the observance of K_2S_2, the coexistence of K_2S_3 in the final discharge product has also been observed [41,42]. Very recently, Lai et al. demonstrated the catalytic oxidation of K_2S_3 resulting in the formation of K_2S as the final product, emphasizing the significance of employing catalytic
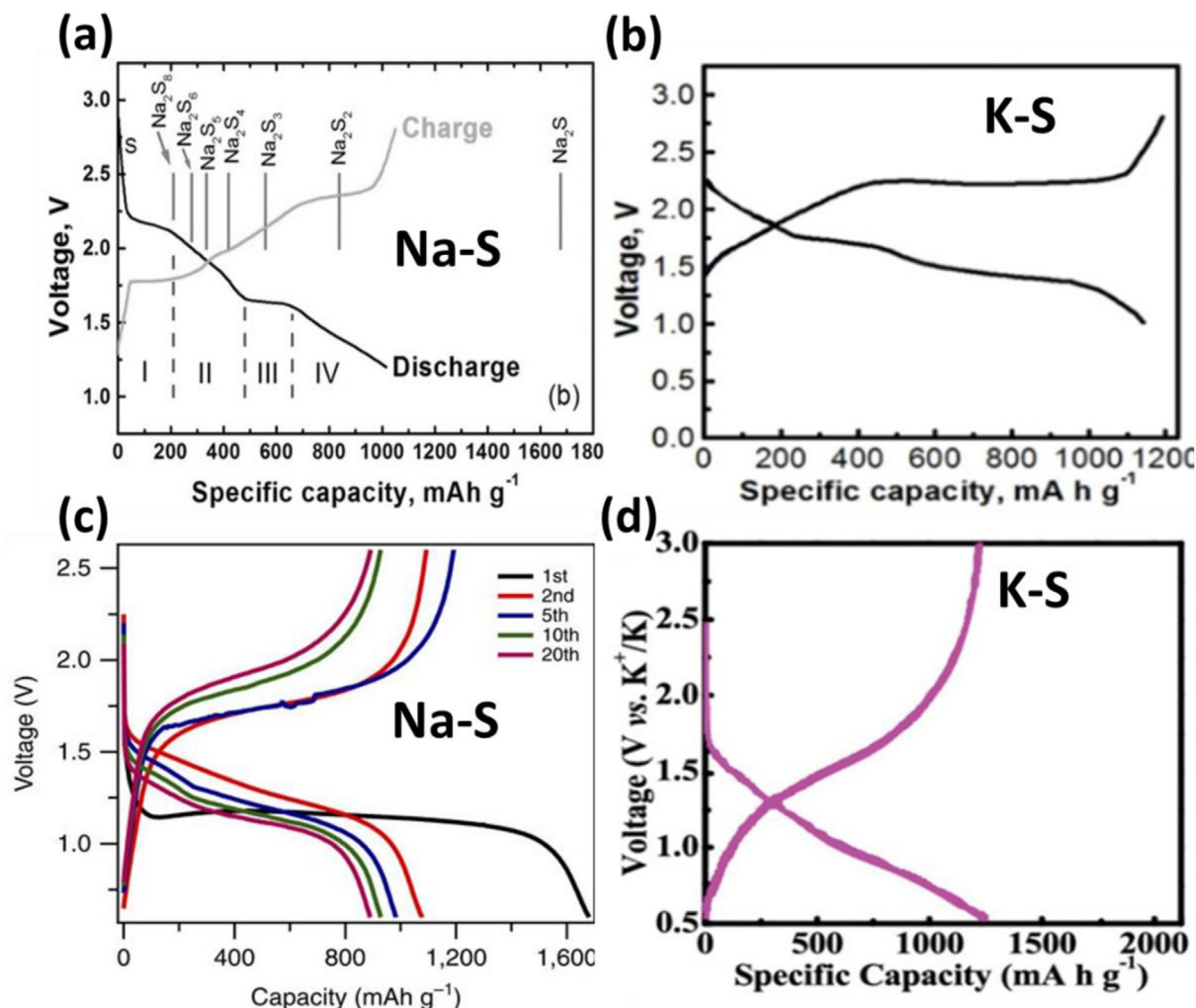
Fig. 3. Typical voltage profiles of (a–b) S_8 species and (c–d) small sulfur molecules or chemically bonded S species in Na–S and K–S batteries. a) Reprinted (adapted) with permission from Ref. [24]. Copyright 2017 John Wiley and Sons. b) Reprinted (adapted) with permission from Ref. [26]. Copyright 2018 Elsevier. c) Reprinted (adapted) with permission from Ref. [25]. Copyright 2013 John Wiley and Sons. d) Reprinted (adapted) with permission from Ref. [27]. Copyright 2019 American Chemical Society.

materials in achieving highly reversible K–S batteries [32]. Currently, diverse materials with catalytic capabilities have been investigated for trapping the poly-sulfide species to improve the reversibility and reaction kinetics of Na–S and K–S batteries. However, the impact of various catalytic materials is different owing to their chemical affinity and reactivity towards the poly-sulfide species. In general, the catalytic materials employed in Na–S and K–S batteries should have the properties such as (1) high conductivity, (2) high adsorption capability, and (3) high catalytic efficiency. When coupled with the low conductivity S active material, the high conductivity catalytic materials can facilitate rapid electron transfer during the electrochemical reaction in Na–S and K–S batteries. Further, the adsorption capability of catalytic materials can ensure that the polysulfide species are effectively adsorbed and aggregated on the catalytic surface mitigating their rampant migration to the anode side. Finally, the effective and complete transformation of polysulfide species can be ensured during the reaction by employing catalytic materials with high catalytic efficiency.

As the design strategies of catalytic materials in both Na–S and K–S systems are analogous and adopt the concept of polysulfide adsorption and catalysis, compositing with a catalytic material adhering to the energy band gap at the molecular level of PS

intermediate species to facilitate effective electron migration pathways is the commonly employed method. Strategies like defect and morphological engineering also accelerates the polysulfide redox process by bringing about PS bond cleavage and precipitation of lower order PS species in the solid phase. The various catalytic materials employed in Na–S and K–S batteries can be categorized basically into four types based on their chemical composition as illustrated in Fig. 4a. Along with the utilization of novel catalysts, the technological advancements have also widened the scope of investigating polysulfide interactions and absorptivity in the recent years with the advances in characterization techniques. Fig. 4b shows the various significant advanced characterization techniques employed in advanced M–S battery systems and the research prospects. The major advances in the employment of engineered catalytic materials and the implementation of advanced characterization in Na–S and K–S batteries are summarized below.

4.1. Transition metal nanoclusters and other dopants

Benefitting from the large surface area, good electroconductivity, high polarity, and unique electron configuration, transition metal-based single-atom catalysts have recently emerged as promising polysulfide catalytic materials. The incorporation of transition metal
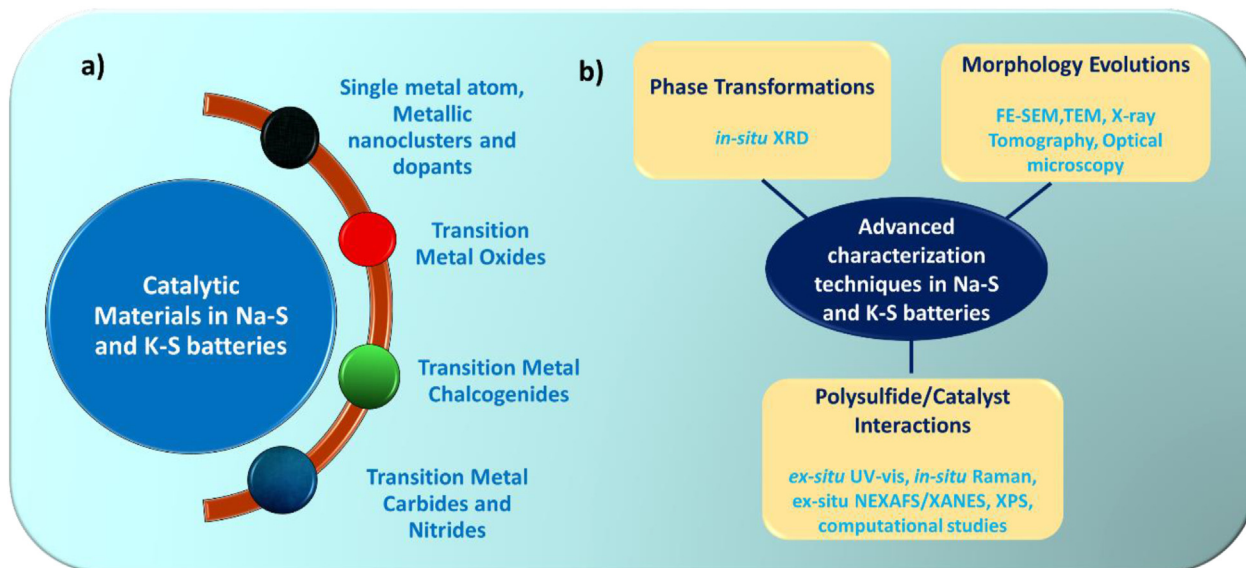
Fig. 4. Schematic of a) various catalytic materials and b) advanced characterization techniques utilized in Na−S and K−S batteries.

nanoclusters has been found exceptionally effective for both polysulfide adsorption and catalytic redox mediation. Amongst the various transition metals, Co-doped carbon structures have shown enhanced electron transfer properties resulting in exceptional performances in M−S batteries [43,44]. Embedding atomic Co atom within hollow carbon sphere as S host (S@Co$_n$-HC) in Na−S cells facilitated fast PS transformation retaining 508 mAh/g at 100 mA/g after 600 cycles [45]. The alleviation of the shuttle effect and electrocatalytic reduction of Na$_2$S$_4$ into Na$_2$S by the atomic Co was demonstrated via a combination of operando Raman spectroscopy, synchrotron X-ray diffraction, and density functional theory (DFT) studies.

Rationally designed conjugated porous polymers, metal-organic frameworks (MOFs), and inorganic compounds have also displayed good polysulfide catalytic capabilities in M−S batteries [46−50]. The synthesis of MOF-derived carbon materials with transition metal nanoclusters benefits from good catalytic absorptivity and the physical confinement within microporous carbons positively influencing polysulfide conversion reactions [51−53]. Similarly, a single Fe atom anchored N-doped mesoporous hollow carbon (NMC) with atomically dispersed dual active sites reported enhanced Na$^+$ ion diffusion coefficients compared to the pristine S electrode (Fig. 5a) [54]. The Fe−N$_4$ sites in the carbon matrix enhanced the chemisorption of polysulfide species via electron (e−) transfer and facilitated excellent Na diffusion to even Na-poor regions, efficiently converting the intermediate polysulfide species to Na$_2$S, unlike that of conventional N-doped carbon cathodes. The coexistence of Na$_2$S$_4$ and Na$_2$S$_x$ at 1.6 V during the discharge process indicates the fast catalytic transformation of polysulfides. Apart from that, the absence of Na$_2$S$_2$ phase indicates the rapid conversion of Na$_2$S$_4$ to Na$_2$S, as evidenced by the synchrotron *in-situ* XRD in Fig. 5b. Such improved reaction kinetics of Na−S cells with Fe−N$_4$ sites resulted in good cycle performances (540 mAh/g after 500 cycles at 100 mA/g). A nano cobalt anchored carbon-wrapped graphene aerogel reported enhancement in the electrochemical reaction kinetics and electric conductivity of the S host [55]. In-situ Raman studies of the S cathode (Fig. 5c and d) during charge/discharge revealed the coexistence of Na$_2$S$_4$, and Na$_2$S$_2$ at 0.5 V and the generation of Na$_2$S species. Further, upon charging, S$_8$ is regenerated at 2.8 V, indicating good active material utilization and fast reaction kinetics. The catalytic oxidation of K$_2$S in K−S cells

was demonstrated by Lai et al. for the first time by a Me-Im solvated Cu^{2+} catalyst leading to unprecedented gravimetric energy of 1779 Wh/kg$_S$ [32]. The strategy of incorporating Me-Im-solvated Cu catalyst resulted in weakening the S−S bond in K$_2$S$_3$ and promoting the rapid formation of K$_2$S. The K−S cells were designed with a liquid phase potassium biphenyl anode which exhibited a high coulombic efficiency (99.9%) along with good capacity retention (84%) over 200 cycles. The correlation between the local electron states of the sulfur cathode in facilitating polysulfides conversion kinetics was reported for the first time by employing a Ni-based 2D MOF as the catalyst [56]. The fast PS transformation kinetics observed in Na−S cells indicated a decrease in electron density for S in the presence of Na$_2$S$_5$. The change in local electron density investigated by near edge X-ray absorption fine structure (NEXAFS) studies carried out on a 2D Ni MOF with Na$_2$S$_5$ revealed a decreased Ni electron density, demonstrated by the increased white-line adsorption energy, from the Ni L-edge spectrum (Fig. 5e), while the C K-edge displayed no electron loss (Fig. 5f). Additional investigations with various PS species revelated that the electron state of the Ni centers is dynamic during discharge/charge processes which corresponded well with the fast conversion kinetics established with Ni-based 2D MOF.

Exploring ZIF-67-derived N-doped Co nanoclusters as a catalytic accelerator in K−S batteries, the impact of the size on catalytic reduction was investigated by Ge et al. recently [57]. Nanoclusters with almost 3 nm Co clusters exhibited superior catalytic activity, ensuring low charge transfer resistance and energy barriers, enhanced current density, and improved conversion reaction rate. An excellent reversible capacity of 453 mAh/g at 50 mA/g after 50 cycles was achieved for this cathode structure. Further, Ye et al. confirmed the influence of Co−S and N−K interactions in K−S batteries via a combination of spectroscopic characterizations, electrochemical evaluation, and theoretical computations [16]. The resulting K−S battery exhibited high capacities of 773 and 535 mAh/g under high current densities of 1 and 2 C, respectively. In-situ synchrotron X-ray diffraction (XRD) measurements (Fig. 6a) confirmed the formation of K$_2$S during the discharge process and revealed that during the charging process, most of the K$_2$S oxidized to polysulfides (>0.5 V), indicating fast kinetics due to the incorporation of atomic cobalt, and thereby contradicted with the argument that K$_2$S can hardly be oxidized during charge. The *ex-*
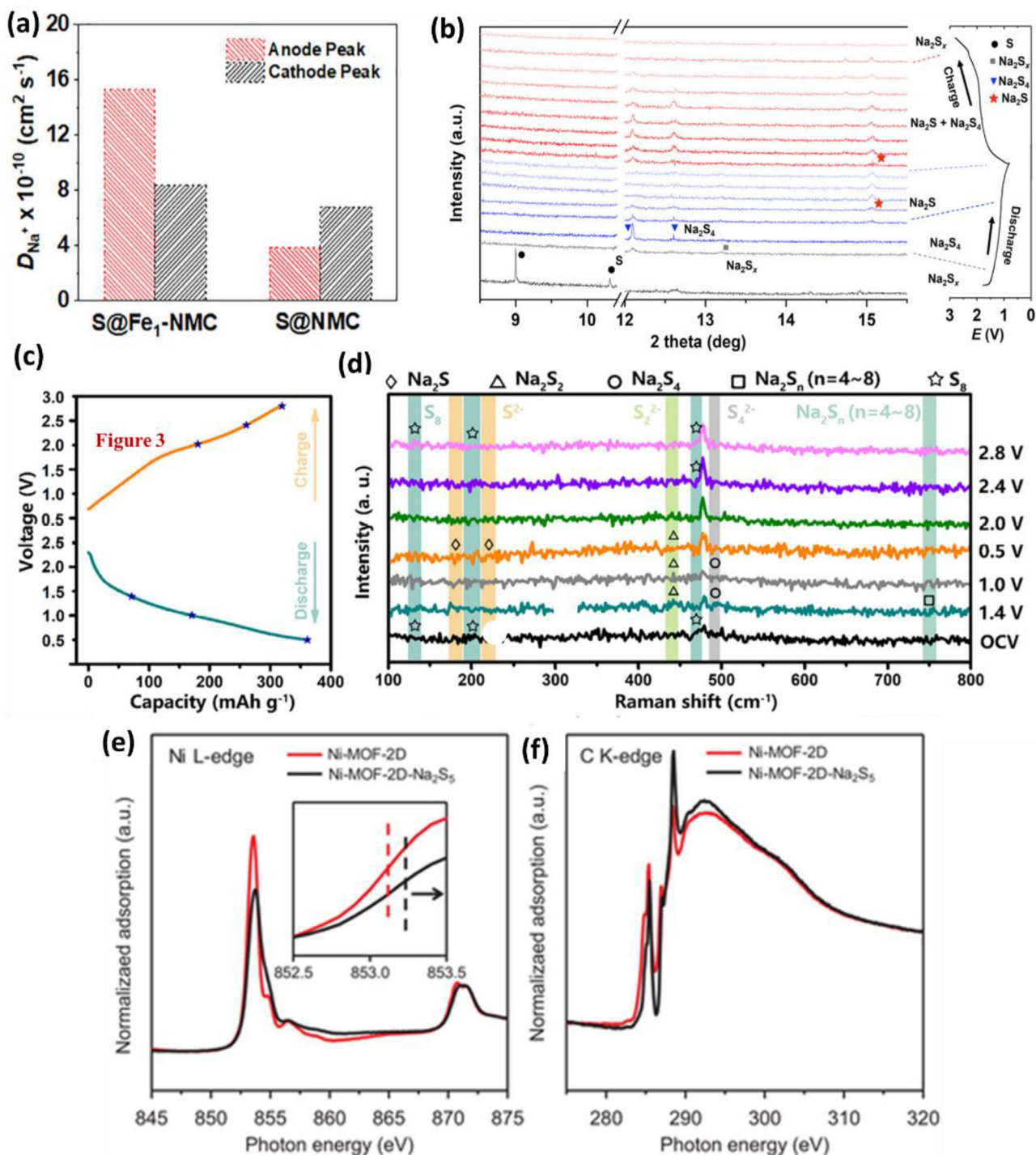
Fig. 5. A) Na$^+$ diffusion coefficients of S@Fe$_1$-NMC and S@NMC, and b) *in-situ* synchrotron XRD results of S@Fe$_1$-NMC cells at various states of charge/discharge. Reprinted (adapted) with permission from Ref. [54]. Copyright 2021 Elsevier. C) schematic illustration, and d) *in situ* Raman analysis of S@Co/C/rGO electrode in Na−S battery at various states of charge/discharge. Reprinted (adapted) with permission from Ref. [55]. Copyright 2020 Elsevier. E) Ni L-edge NEXAFS spectra, and F) C K-edge NEXAFS spectra of Ni-MOF-2D and Ni-MOF-2D-Na$_2$S$_5$. Reprinted (adapted) with permission from Ref. [56]. Copyright 2020 John Wiley & Sons.

situ XPS measurements and the *ab-initio* calculations (Fig. 6b and c) corroborated these findings. The rational design of covalently bonded sulfurized polyacrylonitrile (SPAN) cathodes by doping with non-transition metals has also proven to be effective in improving the reaction kinetics and sulfur utilization in M−S batteries [58–60]. For e.g., Wang et al. employed selenium with high conductivity (1×10^{-5} S/cm) as a dopant in SPAN, which acted as a eutectic accelerator in Na−S. Cells, speeding up the reaction

kinetics and enabling high-rate capability compared to traditional SPAN cells [61]. Similarly, an iodine-doped SPAN electrode demonstrated good reversibility and rate capability in Na−S and K−S cells [62]. The electrode delivered an initial capacity of 1448 mAh/g and an excellent reversible capacity of 722 mAh/g after 100 cycles in K−S batteries. These results indicate the immense scope in engineering sulfur cathodes with suitable dopants for M−S batteries.
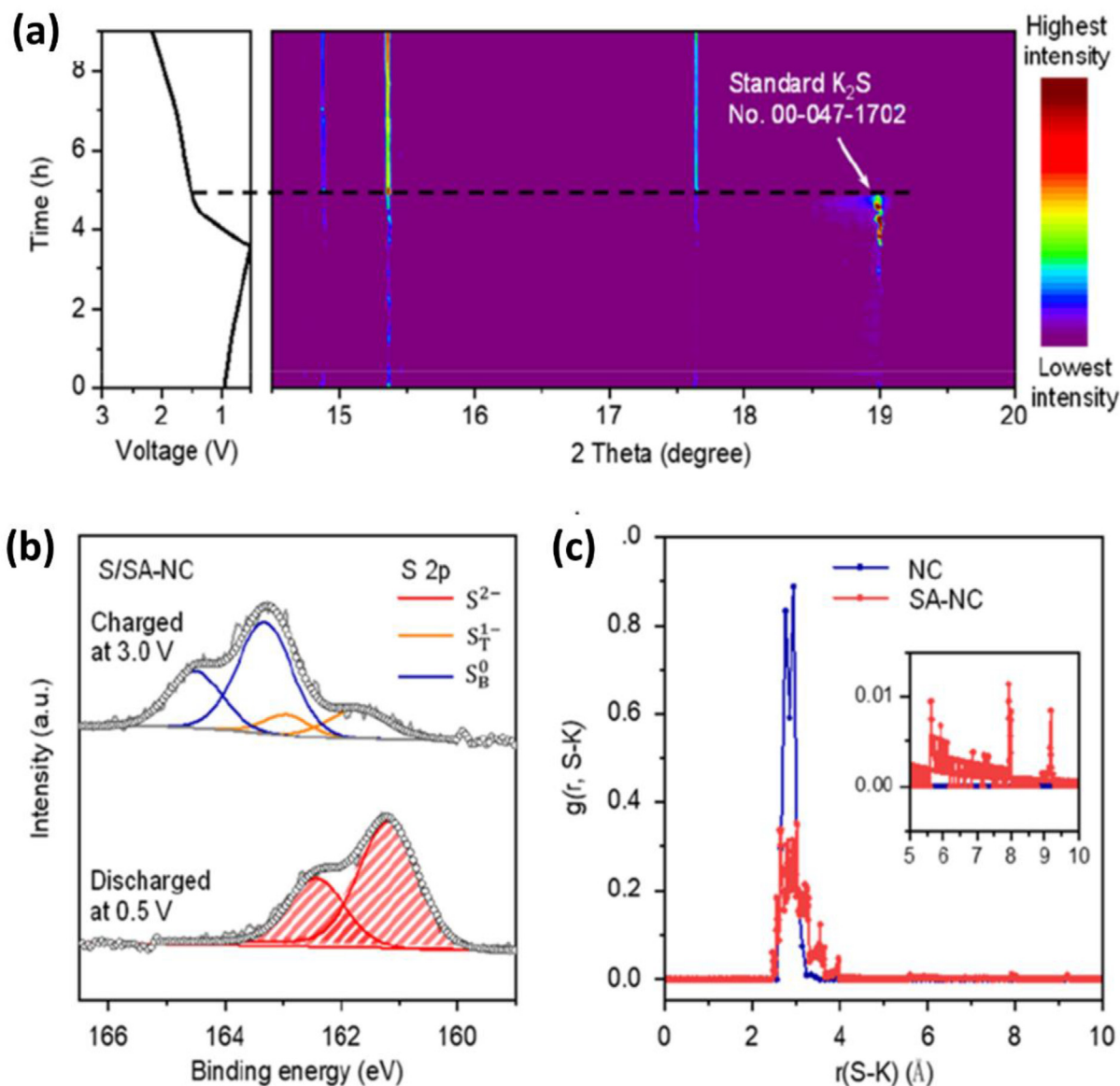
Fig. 6. a) *In-situ* synchrotron XRD patterns for the S/SA-NC electrode in K−S cells. (b) XPS spectra of S/SA-NC electrode and the c) radial distribution function of the S−K bond length calculated by *ab initio* molecular dynamics. Reprinted (adapted) with permission from Ref. [16]. Copyright 2021 American Chemical Society.

4.2. Transition metal oxides

Transition metal oxides are the most versatile catalytic materials employed in M−S batteries owing to their favorable chemical properties, ease of synthesis, low cost, and eco-friendliness [63]. The presence of oxygen anions in them induces strong polar interactions with the polysulfide species leading to the adsorption-catalysis mechanism [64]. Such binding interactions with the polysulfide species can minimize the dissolution of S species into the electrolyte and simultaneously initiate the rapid catalytic conversion of polysulfide species. Various transition metal oxides like TiO_2 [65], MnO_2 [66], Fe_2O_3 [67], and Co_3O_4 [68] have been successfully demonstrated as efficient electrocatalysts and polysulfide adsorbers in Li−S batteries. Subsequent investigations on the catalytic activity of transition metal oxides in Na−S and K−S batteries have also garnered immense research interest recently.

An *in-situ* grown vanadium dioxide (VO_2) nanoflower catalyst on rGO (Fig. 7a) reported 156.1 mAh/g after 1000 cycles at 2C, exhibiting 0.07% capacity decay per cycle [69]. The natural polar nature of VO_2 nanoflowers aids in trapping the polysulfide species. At the same time, the catalytic effect of VO_2 leads to the accelerated conversion of long-chain NaPS species to Na_2S compared to the bare rGO substrate with weak adsorption capability. In another work, the catalytic adsorption and mitigation of PS shuttling in a NaPS battery was demonstrated with free-standing. MnO_2 decorated carbon cloth. The system consisted of a catholyte active material (Na_2S_6) and demonstrated good catalytic adsorption and rapid conversion of polysulfide species due to the *in-situ* formation of a polythionate complex, mitigating the dissolution in electrolyte [70]. Fig. 7b shows the $Mn2p_{3/2}$ XPS spectra of both $CC@0.5MnO_2@Na_2S_4$ and $CC@0.5MnO_2@Na_2S_6$ samples revealing the reduction of Mn^{4+} species to Mn^{3+} and Mn^{2+} with the introduction of polysulfide species. This result confirms the existence of
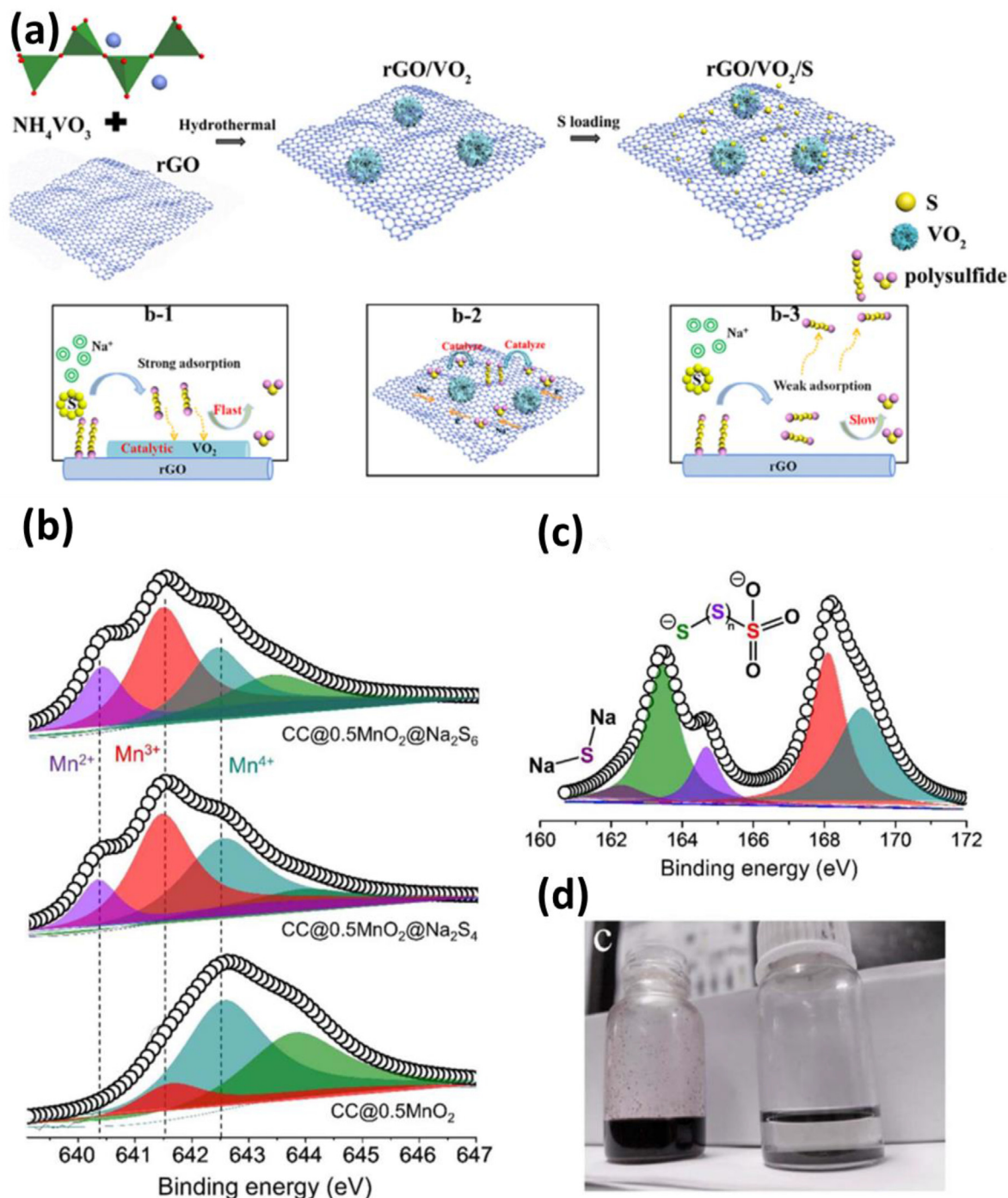
Fig. 7. a) Schematic illustration of the synthesis of rGO/VO$_2$/S composite and its advantages. Reprinted (adapted) with permission from Ref. [69]. Copyright 2019 Elsevier. b) Mn 2p3/2 spectra of CC@0.5MnO$_2$, CC@0.5MnO$_2$@Na$_2$S$_4$, and CC@0.5MnO$_2$@Na$_2$S$_6$, c) S 2p3/2 spectrum of CC@0.5MnO$_2$@Na$_2$S$_6$ and d) digital photograph showing the variation of the polysulfide solution with the addition of MnO$_2$ catalyst, in polysulfide solution. Reprinted (adapted) with permission from Ref. [70]. Copyright 2019 Elsevier.

a catalytically favored surface redox reaction between MnO$_2$ and Na$_2$S$_n$. The S2p$_{3/2}$ XPS spectra of CC@0.5MnO$_2$@Na$_2$S$_6$ (Fig. 7c) also validated the formation of polythionate complexes containing thiosulfate group arising from the redox reaction of MnO$_2$ and Na$_2$S$_n$. The polysulfide adsorption was also visually verified with the addition of MnO$_2$ catalyst, in polysulfide solution (Fig. 7d). A modification of this work consisting of CC@MnO$_2$ NaPS host with

sodium–alginate nanofibers also demonstrated the advantages of catalytic redox mediation and PS adsorption [71]. Furthermore, low temperature (−10 °C) cycling of NaPS cells consisting of a hybrid cathode consisting of indium tin oxide nanoparticle decorated activated carbon cloth demonstrated by the same group showed excellent advancements in cycle performances [72]. The ex-situ XRD of the fully discharged Na$_2$S$_6$@ITO@ACC electrode after 1000

cycles revealed the coexistence of both Na_2S_2 and Na_2S phases. However, the presence of Sn−S bond between ITO and the Na_2S_n species was confirmed from the *ex-situ* XPS measurements indicating strong confinement of the polysulfide species.

Many recent studies have put forward rational design strategies embedding catalytic materials in separators and interlayers to improve the electrochemical performances of M−S batteries. For e.g., a modified separator incorporating an Al_2O_3−Nafion membrane on a glass fiber separator also demonstrated the advantage of the PS adsorption capability of Al_2O_3 and the ion selectivity of Nafion membrane repelling the polysulfide anions (S_n^{-2}) owing to the negatively charged sulfonic group while allowing Na^+ ions transport through them [73]. An interlayer consisting of MoO_3 as a catalytic redox mediator was reported to enhance the reaction kinetics of Na−S cells along with simultaneously reacting with NaPS species to form thiosulfate/polythionate complexes. The interlayer configuration could effectively inhibit polysulfide dissolution, as evidenced by post-cycling UV−vis spectroscopy studies of the electrolyte [74]. In a similar work, a V_2O_3/CNF interlayer demonstrated excellent active material utilization (70%) at 0.1C rate [75]. High-resolution XPS spectra after cycling indicated significant changes in V_{2p} and S_{2p} spectra, indicating NaPS adsorption and conversion of higher-order NaPS to lower-order NaPS by forming $S_2O_3^{2-}$ groups. Yuan et al. reported electrospun SPAN nanofibers embedded with a bimetallic transition metal oxide, Fe_xNb_yO with high electrochemical activity, high sulfur utilization, and high cycling stability in K−S batteries [76]. The free-standing FeNb@-SPAN composite cathode featuring interwoven nanofibers with Fe_xNb_yO nanoparticles catalyzed the reaction apart from accommodating the volume expansion and mitigating polysulfide dissolution during potassiation/depotassiation. An outstanding energy storage performance of 776 mAh/g under 50 mA/g was demonstrated for this electrode structure via electrocatalysis. In general, the NaPS binding strength in various oxides is determined by the amount of charge transfer from S atoms to O atoms. The strong interaction between sodium and oxygen atoms in an amorphous silica incorporated S host was elucidated via MD simulation and first-principles calculation studies [77]. The formation of Na−O chemical bonds between amorphous silica and sodium polysulfides that led to favorable NaPS binding was established clearly, substantiating the good reversible capacities achieved despite the high S loading in the work.

4.3. Transition metal chalcogenides

Transition metal chalcogenides (sulfides and selenides) possess good electronic and catalytic properties and are of sufficient interest in M−S batteries due to their polar nature and interaction with polysulfides [78]. The weak M−S bonds in transition metal sulfides compared to the M−O bonds in transition metal oxides also help to facilitate rapid catalytic redox reactions in M−S batteries [79]. Transition metal sulfides as electrocatalysts in Li−S batteries (MoS_2, $FesS_2$, NiS_2, VS_2, CoS_2, etc.) also benefit from good electrical conductivities compared with their oxide counterparts [79]. This manifests as fast electron transfer properties during the catalytic conversion of polysulfides and improves the utilization of active sulfur in the electrode. In another attempt, to improve the conductivity and catalytic adsorption of polysulfides in Na−S batteries, Luo et al., designed sulfur deficient flower-like MoS_{2-x}/C composite spheres and interlayer-enlarged MoS_{2-x} nanosheets confined within hollow carbon nanospheres (FL-MoS_{2-x}@HC) with abundant active sites [52]. The improvement in the adsorption/catalysis mechanism via the introduction of sulfur vacancies in MoS_2 was also successfully verified via first-principles calculations. The confinement of polysulfides was validated by visually observing the

change in the colour of the polysulfide solution after soaking FL-MoS_{2-x}@HC for 2 h (Fig. 8a). Additionally, the reduction in the intensity of the characteristic peaks of NaPS species in UV−vis absorption tests (Fig. 8b) also confirmed the excellent polysulfide adsorption capability of the composite.

Transition metal selenides possess high electronegativity and strong interactions with polysulfide species on account of their polar nature, similar to that of transition metal sulfides [80]. Especially 2D selenides have been proven to have narrower band gaps, higher conductivity and faster electron transfer rates, than their oxide and sulfide counterparts [81]. The catalytic absorptivity and interaction of a 2D $MoSe_2$ electrocatalyst with polysulfide was demonstrated in Na−S cells by conducting XPS studies of the $S2p_{3/2}$ spectra of 2H−$MoSe_2$/N-HCS soaked with Na_2S_6 solution [82]. The shifting of binding energies to the lower end after introducing 2H−$MoSe_2$/N-HCS (Fig. 8c) revealed the existence of strong chemical interaction between Na_2S_6 species and $MoSe_2$.

The confinement of short-chain sulfur in tailored larger pores (>0.5 nm) has been another strategy to mitigate polysulfide dissolution and shuttling in M−S batteries [85,86]. This strategy was combined with the catalytic conversion of polysulfide species with a CoS_2 electrocatalyst in Na−S batteries by Xiao et al. [83] The resultant Na−S cells exhibited excellent long-term cyclability retaining 403 mAh/g after 1000 cycles. The high adsorption energy of CoS_2 compared to the N-doped carbon (Fig. 8d) calculated via DFT studies revealed strong interaction of CoS_2 with the polysulfide species, resulting in excellent confinement. The visual adsorption test and UV−vis measurements of the supernatant of the CoS_2/NC-soaked polysulfide solution also confirmed the complete adsorption of polysulfide species. In a similar attempt, a hybrid coating layer consisting of FeS_2/C nanocubes and conductive CNT prepared on GF separators by vacuum filtration in combination with the yolk shelled hollow FeS_2/C nanocubes was reported as a dual polysulfide defense strategy by Wang et al. [84] Interestingly, the high S loading cathode (7.6 mg/cm^2) retained an ultralow capacity decay rate (0.024%) even after 1000 cycles. The XRD patterns obtained during the initial charge/discharge process (Fig. 8e and f) confirmed the gradual transformation of higher-order polysulfides to lower-order polysulfides resulting in the formation of Na_2S upon discharging to 0.8 V. However, the absence of Na_2S_2 phase upon complete charge indicated rapid catalytic transformation of Na_2S_2 by the interaction of the polar catalyst FeS_2. DFT studies have demonstrated high binding energies for the interaction of Na_2S with NiS_2 compared to N-doped carbon nanotubes indicating their high polysulfide adsorption capability. The strong binding of NiS_2 to Na_2S translates to the rapid conversion of Na_2S_4 into Na_2S, mitigating polysulfide dissolution and ensuring efficient active material utilization in Na−S cells. SeS_x-based solid solutions have been thoroughly investigated in M−S batteries due to improved ion/charge transfer properties acquired by the incorporation of conductive selenium (1×10^{-3} S/m) with the non-conductive sulfur [58,87,88]. Investigation of a SeS_2/SPAN composite consisting of covalently bound SeS_2 explored for both Na−S and K−S batteries revealed good long-term cyclability on account of the one-step conversion without the formation of soluble polysulfides and polyselenides [89].

4.4. Transition metal carbides and nitrides

Transition metal carbides and nitrides are low cost, polar materials that exhibit excellent performance as electrocatalysts in M − S batteries, accelerating the redox kinetics of polysulfide conversion [90]. Among them, transition metal carbides have been reported to display dual effects of both adsorbing the PS species and accelerating the redox kinetics of the PS transformation in Li−S batteries [90]. Inspired by these, similar strategies have been
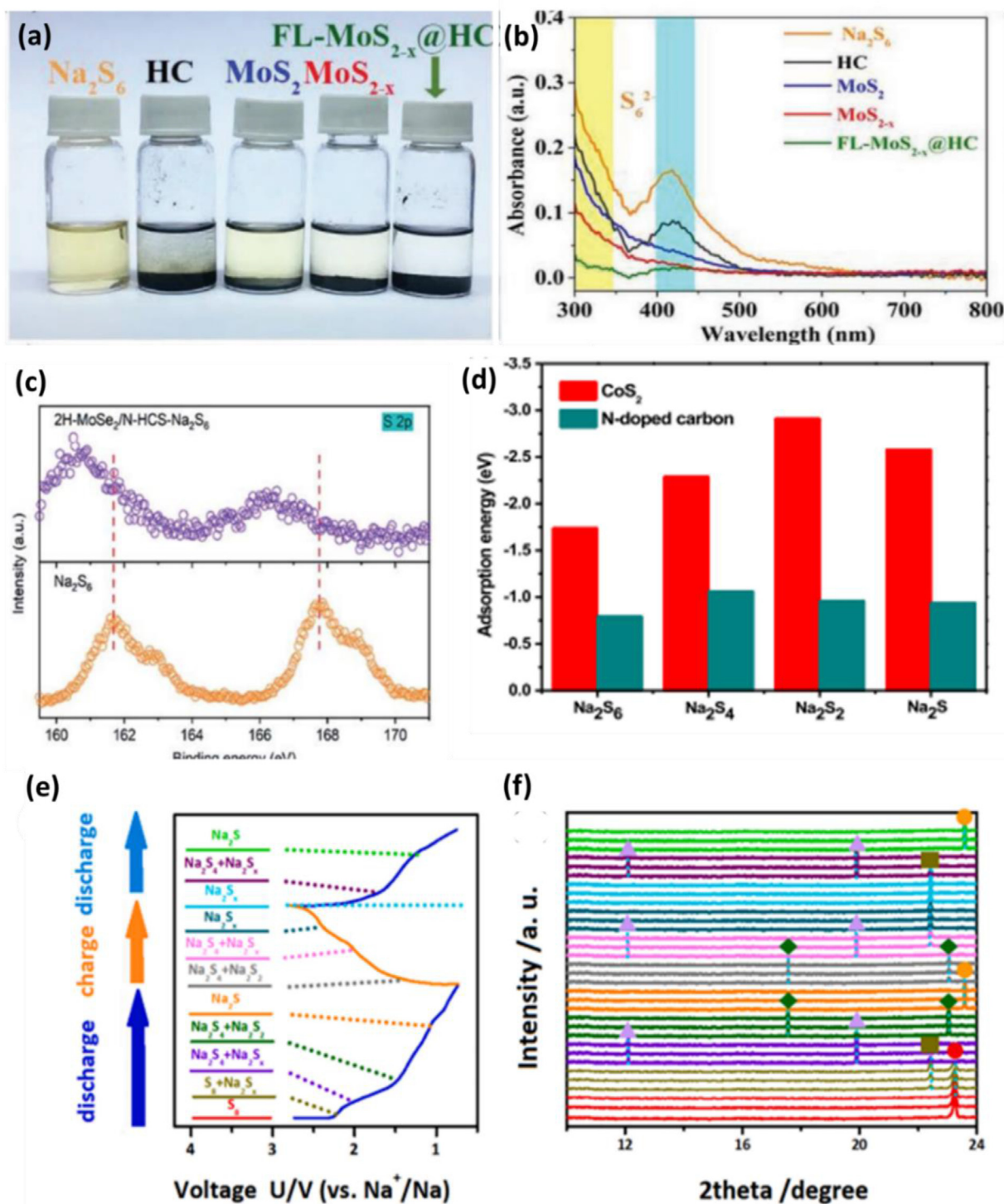
Fig. 8. a) Photographs of polysulfide adsorption tests with and without addition FL-MoS$_{2-x}$@HC, and the corresponding b) UV−vis spectra of taken after 2 h. Reprinted (adapted) with permission from Ref. [52]. Copyright 2021 John Wiley & Sons. c) comparison of high-resolution XPS spectra of S 2p for pristine Na$_2$S$_6$ and 2H−MoSe$_2$/N-HCS + Na$_2$S$_6$. Reprinted (adapted) with permission from Ref. [82]. Copyright 2020 Royal Society of Chemistry. d) comparison of adsorption energies of Na$_2$S$_x$ species on CoS$_2$ and N-doped carbon. Reprinted (adapted) with permission from Ref. [83]. Copyright 2021 American Chemical Society. e) charge/discharge curves and f) corresponding *ex-situ* XRD patterns in FeS$_2$ core-shell hybrid fiber cathode. Reprinted (adapted) with permission from Ref. [84]. Copyright 2021 Elsevier.

adopted to improve the cyclability of Na−S batteries. One such study involves the case of a polar hybrid structure reported by Qin et al., consisting of Co$_3$C−Co with fluorinated carbon nanotubes arrays encapsulated in a porous three-dimensional framework (FCNT@Co$_3$C−Co) that demonstrated strong interaction with NaPS,

suppressing their dissolution in the electrolyte [91]. Visual and UV adsorption tests further confirmed the adsorption of NaPS onto this hybrid structure. The hybrid design benefitted from both chemical and physical adsorption of polysulfide species, improving the long-term cyclability of cells. Despite their unique functionality and low

cost, not many work has been reported on the catalytic effects of carbide materials in advanced M−S batteries which possess huge prospects for fundamental research and applications.

The distinctive electronic structure, high electronic conductivity, and excellent selectivity of transition metal nitrides (TMNs) are known to render remarkable catalytic activity [92,93]. A theoretical investigation of the interactions of various TMNs with lithium polysulfides revealed strong polysulfide binding capability compared with carbonaceous materials and TMSs [94]. In Na−S batteries, TMNs have not been investigated in detail. A recent report on the investigation of Mo_xN_y catalysts (Mo_5N_6, MoN, and Mo_2N) with carbon-sulfur composites revealed excellent electrodeposition and kinetics [95]. The composite with Mo_5N_6 electrocatalyst was reported to have a remarkable cycle life of 10,000 cycles under 1C (1675 mA/g). The *ex-situ* synchrotron-based near-edge X-ray absorption fine structure characterizations (Fig. 9a) revealed a consistent decrease in the valence state of Mo upon discharge, indicating strong Mo−S interaction and high Na_2S electrodeposition capacity. The gradual increment to the original state upon charging further confirmed the strong electrocatalytic nature. Additional investigations on the absorbability on Mo_5N_6 surface carried out via density of states computational studies indicated low Na_2S_2 dissociation free energy due to its high d-band position in Mo_5N_6. This was found to accelerate the Na_2S

electrodeposition in Mo_5N_6 compared to the other nitride counterparts. In another attempt, boron nitride incorporated polymeric membrane employed as a blocking interlayer in Na−S cells exhibited strong NaPSs confinement via chemisorption [96]. Significant improvement in capacity retention (83.1% at the end of 500 cycles) was demonstrated compared to cells without an interlayer, suggesting the utility of catalytic materials via novel interlayer configurations. In a recent study, Huang et al. reported a bifunctional sheath of $Fe(CN)_6^{4-}$-doped polypyrrole sheath as a cation reservoir and polar redox mediator that promotes the polysulfide conversion in Na−S cells [97]. The electrocatalytic redox Fe centers in $Fe(CN)_6^{4-}$ were found to lower the Na_2S activation energy barrier enabling the high reversibility of Na_2S electrodeposition. The quasi-solid-state reduction pathway investigated with *in-situ* Raman and *ex-situ* XRD studies (Fig. 9b and c) revealed the complete catalytic conversion of Na_2S_4 to Na_2S upon discharge. The Na−S cells displayed good reversibility due to the existence of $Na_4Fe^{(II)}(CN)_6$/ $Na_3Fe^{(III)}(CN)_6$ redox mediator that successfully catalyzed the conversion of polysulfides.

The synergistic catalytic effect of metal nitrides and oxides was explored in a recent study of sulfur cathodes consisting of $TiN−TiO_2$ heterostructures encapsulated in multichannel carbon fibers [98]. Visual adsorption experiments of these heterostructures with Na_2S_6 carried out by soaking for 2 h revealed that the polysulfide
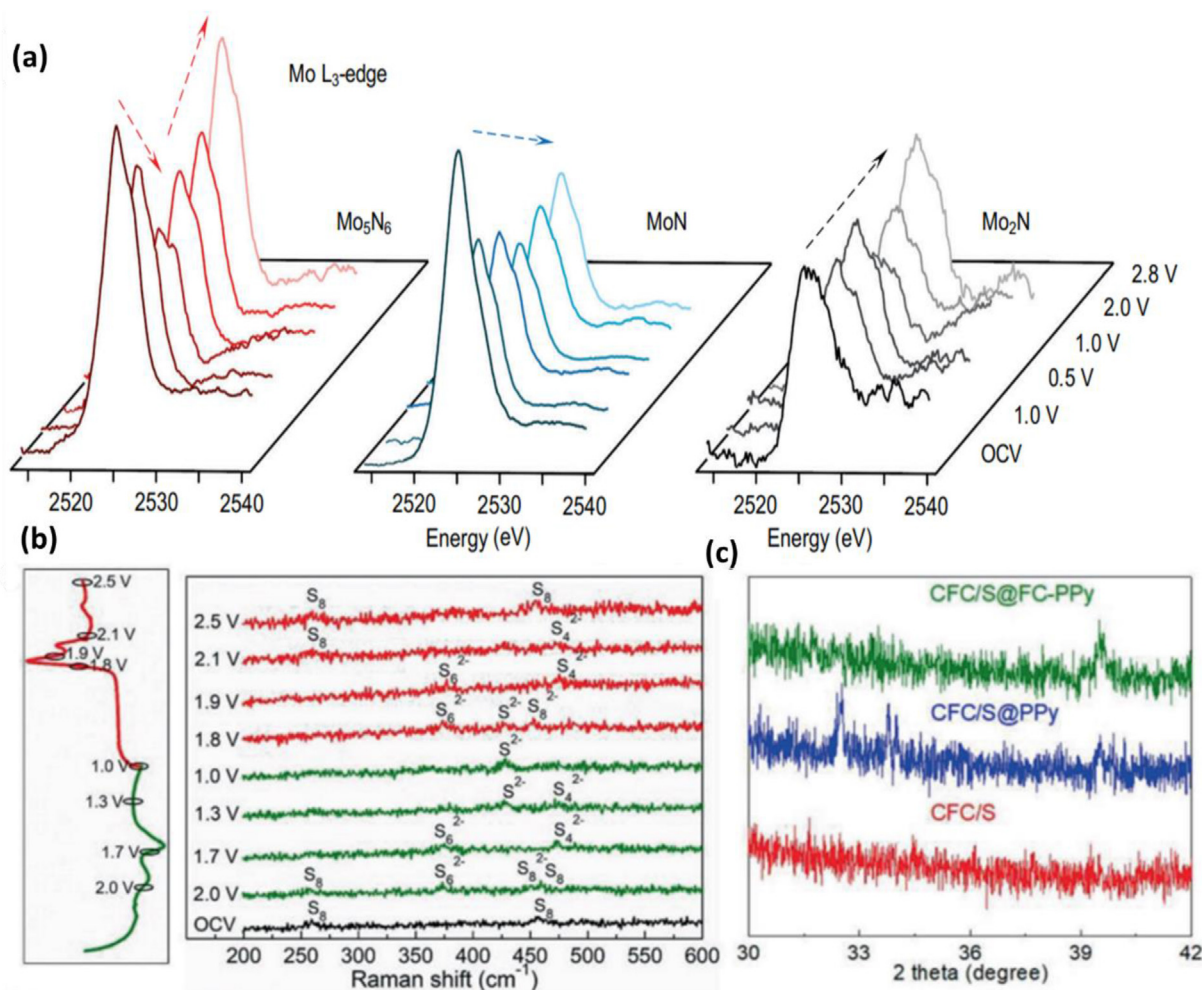

Fig. 9. a) *Ex-situ* NEXAFS for the Mo-L_3-edge of S/Mo_5N_6, S/MoN, and S/Mo_2N during a discharge/charge process. b) cyclic voltammogram with the test potentials for analysis and the *in-situ* Raman spectra of CFC/S@FC-PPy, and c) *ex-situ* XRD patterns of sulfur cathodes in fully discharged state. Reprinted (adapted) with permission from Ref. [97]. Copyright 2021 John Wiley & Sons.

solution containing TiN−TiO$_2$ heterostructures and TiO$_2$ turn transparent, indicating the strong adsorption capability (Fig. 10a). Further, investigation of Na$_2$S nucleation and growth carried out via Na$_2$S precipitation studies revealed the highest Na$_2$S precipitation capacity for the TiN−TiO$_2$ incorporated heterostructure. The rapid conversion of polysulfides to Na$_2$S was confirmed by the Na$_2$S deposition curves (Fig. 10b−e), and the visual adsorption tests indicated robust electrocatalytic conversion to polysulfides compared with TiO$_2$.

MXenes are a new family of a few atoms thick, two-dimensional (2D) inorganic compounds (transition metal carbides, nitrides and carbonitrides) with the general formula, M$_{n+1}$X$_n$T$_x$ where M is a transition metal such (Ti, Cr, V, Mo, Nb, etc.), X can be carbon or nitrogen, and T$_x$ indicates the terminal functional group (F, O, and OH). They have attracted broad research interests as a promising class of 2D materials with versatile applications in catalysis and energy storage [99−102]. The presence of active functional surfaces, high electronic conductivity, and chemical durability favor their applications in M−S batteries. MXene-based dendrite-free K−S batteries were reported by incorporating potassium metal into

a titanium-deficient nitrogen-containing MXene/carbon nanotube scaffold with potassium-philic characteristics [103]. The defect-engineered MXenes could successfully induce the nucleation of K atoms, suppress the dendritic growth, and protect the K-metal from the detrimental effects of polysulfide shuttling.

S-atom doped MXenes (S−Ti$_3$C$_2$T$_x$) possess enhanced redox reactivity of Na−S and offer controlled diffusion of polysulfides into the electrolyte [104]. The preferential binding of NaPS species to the surface of the S−Ti$_3$C$_2$T$_x$ compared to that of O−Ti$_3$C$_2$T$_x$ or F−Ti$_3$C$_2$T$_x$ was validated by DFT studies. This finding corroborates well with polysulfide shuttle-free operation and the long-term cyclability of Na−S cells. In a similar attempt, N-doped Ti$_3$C$_2$T$_x$ MXene microspheres were also reported to exhibit a strong affinity to NaPSs via Na−N and Ti−S interactions resulting in highly efficient binding toward NaPS [105]. Raman studies of the electrodes after discharge further confirmed the polysulfide adsorption capability of N−doped Ti$_3$C$_2$T$_x$ nanosheets (Fig. 10f). Subsequently, a self-discharge test of the cell with N−doped Ti$_3$C$_2$T$_x$ nanosheets revealed better retention of open circuit voltage (2.36 V for 50 h) than that of bare MXene cell which exhibited fast degradation
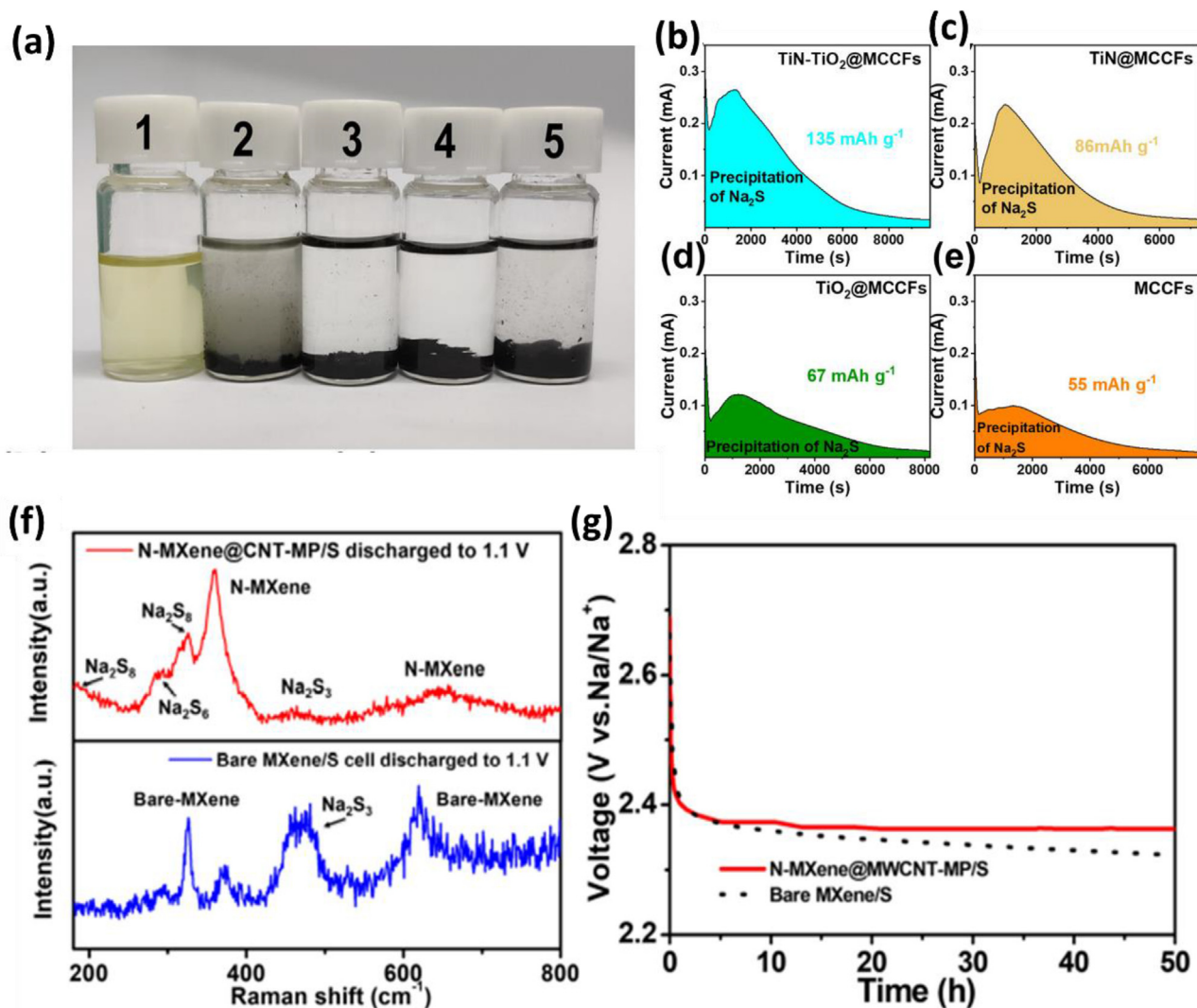

Fig. 10. a) Photographs of polysulfide with the addition of MCCFs, TiN@MCCFs, TiN−TiO$_2$@MCCFs, and TiO$_2$@MCCFs and b-e) the corresponding potentiostatic discharge curves of Na$_2$S$_6$/EC/PC solution on various surfaces. Reprinted (adapted) with permission from [98]. Copyright 2021 American Chemical Society. f) Raman spectra of N− N-doped Ti$_3$C$_2$T$_x$ MXene microsphere and Ti$_3$C$_2$T$_x$ incorporated sulfur cathodes after 1000th cycle, g) self-discharge static test of N-MXene@MWCNT-MP/S coin cell. Reprinted (adapted) with permission from Ref. [105]. Copyright 2021 American Chemical Society.
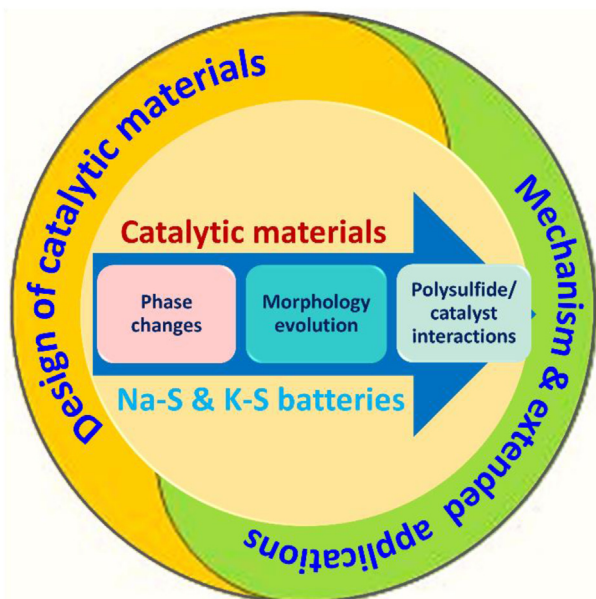
Fig. 11. Schematic outlook on the design and development of catalytic materials Na—S and K—S batteries.

(Fig. 10g). The slow degradation of open circuit voltage in the cells with N-doped $Ti_3C_2T_x$ MXene microspheres confirmed the strong catalytic binding and prohibition of high-order sodium polysulfide diffusion.

5. Conclusions & perspectives

The Na—S and K—S battery systems hold great promise from the perspective of high energy density and cost-effectiveness, which is expected to be suitable for large-scale energy storage. However, the commercialization of these systems is impeded by the sluggish redox kinetic and the shuttling of polysulfides. The slow conversion kinetics of sulfur species is identified as the factor for the shuttle effect, leading to poor energy output and cycling life. The application of catalytic materials on the sulfur cathode is a promising solution strategy, which can effectively capture the sulfur species and catalyze the conversion process. In this review, the design and modification strategies of various catalytic materials for Na—S and K—S batteries have been summarized and analyzed. First, the sodium and potassium storage mechanism in sulfur is discussed, and the significance of catalytic materials in improving the electrochemical performances in these systems is emphasized. Additionally, the role of heteroatom-doped carbon, transition metals, and metal compounds in establishing a synergistic effect of adsorption and catalysis in these systems to alleviate the shuttle effect is elucidated. So far, catalytic materials have shown excellent prospects in accelerating sulfur redox kinetics. However, many aspects are left to be investigated both in the design and development of catalytic materials and their impact on the redox pathways in Na—S and K—S batteries. The prospects and future of these advanced M—S battery systems are also discussed in the light of advanced in-situ characterization techniques.

The catalytic reaction is an electrochemical reaction that catalyzes the redox process of the sulfur cathode, which can enhance the conversion kinetics of sulfur species. However, the surface property changes of the catalytic material after accelerating the electrode reaction have not been explored clearly, unlike conventional catalysts. In the future, it is imperative to study the structural changes of catalytic materials during the reaction. An in-depth

understanding of the catalytic principles for the conversion of sulfur species is pivotal for designing catalytic materials. Considering the complexity of the conversion process associated with sulfur species, it is critical to explore the sodium/potassium-ion storage mechanisms and catalytic process with the help of various characterization methods, such as theoretical calculations and *in-situ* characterization techniques like *in situ* synchrotron X-ray absorption (XRD), Raman and transmission electron microscope (TEM). Combining different characterization methods to verify the catalytic activity of catalytic materials from different viewpoints is of great significance in analyzing catalytic mechanisms and the design of catalytic materials. Fig. 11 encompasses the schematic outlook on design/development of catalytic materials and their ability to tune the reversibility of Na—S and K—S batteries.

Though the development of catalytic materials to solve the intrinsic issues of Na—S and K—S batteries is regarded as one of the most promising strategies, the design and application of catalytic materials are still not well established. There are so many challenges that need to be addressed to understand the impact of catalytic materials on tuning the reversibility and cyclability of these advanced M—S battery systems. For e.g., the precise construction of metal atom doping sites and coordination geometry has not been achieved so far. Alternatively, the impact of the finetuning of the dopant ratios also requires systematic scientific study. Solutions to these problems are restricted because of the randomness of binding sites in carbon supports. Most currently reported catalysts still require further optimization by tuning the atomic metal-carbon structures to enhance the catalytic efficiency and stability simultaneously. Due to this, the design of catalytic materials with homogeneous sites coordinating with heteroatoms is highly desired. On the other hand, metal nanoparticles on carbons usually exhibit insufficient binding ability or undergo reconstruction of chemical compositions, thus resulting in inferior long-term cycling stability. To date, carbon-supported metal oxides have demonstrated robust chemical interaction with polysulfides and can capture them to relieve the shuttle effects. However, the catalytic activities of many reported metal oxides are still not satisfactory. Therefore, exploring new metal oxide-based catalysts with better performance is anticipated to facilitate high-performances. When compared with transition metal oxides, sulfides and nitrides are comparatively good catalysts to accelerate the reaction kinetics though their adsorption capability is weak. It is critical to explore these potential electrocatalysts and determine the limiting factors in improving the reaction kinetics.

Additionally, sulfurization and phosphorylation of metal oxides lead to improved interfacial electron transfer dynamics positively influencing the catalytic properties. It is essential to investigate the binding energy of the resultant sulfides/phosphides with the respective polysulfide species. Such studies can be beneficial in understanding the precise impact of novel catalytic materials on polysulfide adsorption. Probing the influence of such catalytic materials by quantifying the rate kinetics of the polysulfide conversion reaction and understanding the limiting factors would be a great challenge, which could inevitably revolutionize the design prospects of catalytic materials. The possible Na^+/K^+ intercalation into such electrochemically active catalytic materials is also a factor that should be considered and investigated in detail to determine the aspect of capacity contribution arising from them. In such instances, it is critical to design and optimize the voltage window of operation and content of electrochemically active catalytic materials in Na—S and K—S batteries to suit specific applications.

Metal atom doping and simultaneous construction of hierarchical/hybrid/hetero-structures can be beneficial to optimize the surface/interface electronic structure of TMOs, TMSs, TMSes, TMCs and TMNs. This can render unique electronic and bifunctional redox properties for such transition metal-based alloys and make

them promising candidates for achieving high activity and robust stability in M−S batteries compared to their monometallic components.

Na−S and K−S batteries require an efficient flow of electrons, and hence the electrical conductivity of the supporting matrix (on which the metal oxides are loaded) also plays a critical role in promoting efficient catalysis. Additionally, the hetero atom-doped metal oxides, including N, S, P, and other metals, should also be considered for tuning the electronic structures of the catalysts. Thus, to achieve high reversibility and long-term cyclability in Na−S and K−S batteries, the rational design of polysulfide catalytic materials with active site-loaded porous carbons promotes electrocatalysis of polysulfide species, and acceleration of reaction kinetics is crucial. Apart from that, the investigation of direct polysulfide conversion from long-chain to short chain polysulfides by controlling the molecular structure of the polysulfide species with catalytic materials would be very exciting and beneficial. Such strategies can alter the reaction pathways in Na−S and K−S batteries leading to better performances and efficiency.

The evolution of phase transitions during the complex polysulfide transitions at various states of charge and discharge can often provide critical insights into the reaction mechanisms. Apart from the traditional characterization techniques, *in-situ/operando* XRD studies have been employed to monitor and understand such phase transformations during the reactions in real time. Such direct observations of polysulfides by XRD have been able to provide evidence for the polysulfide conversion mechanisms in Na−S and K−S cells. Similarly, the employment of electron microscopy techniques (TEM, field emission scanning electron microscopy (FE-SEM)) has been advantageous in probing the nanoscale changes occurring in the morphology of the sulfur electrodes during the charge/discharge process. In that regard, *in-situ* TEM enables real-time recording of structural evolutions and changes in chemical compositions within the electrode structure with high spatial resolution. The effective detection of the long chain polysulfides has been made possible by employing *in-situ* Raman spectroscopy. On the other hand, UV−vis spectroscopy is a simple yet versatile technique widely used to distinguish the specific polysulfide species generated during the reaction process in M−S batteries. Apart from these, understanding the evolution of interfacial chemical properties of the sulfur electrodes during electrochemical reactions is also critical to outline the reaction mechanisms during charge/discharge. This can be successfully investigated by investigating the resultant chemical states involved electrode active materials via XPS studies. Nevertheless, the amorphous nature of intermediate polysulfides has added significant challenges to the investigation of reaction mechanisms in advanced M−S batteries. Though NEXAFS studies have already demonstrated the correlation of local electron densities observed in the S cathode in achieving improved reaction kinetics with the addition of catalytic material, the detection of specific amorphous solid phases and polysulfide species with NEXAFS/X-ray absorption near edge structure (XANES) investigations has the potential for altering the course of research in advanced M−S batteries. X-ray tomography is another powerful tool that can reveal unique information on material redistribution or conversion via 3D images in complex electrochemical systems like Na−S and K−S by recording images of the region of interest. *In operando* X-ray tomography studies in combination with *ex-situ* characterization can shed light on the formation of specific solid polysulfide intermediates in Na−S and K−S systems which is of significant research interest. Though the employment of these advanced characterization techniques has elevated the research prospects in Na−S and K−S batteries, it is imperative to utilize and creatively modify the conventional chemical or physical analytical techniques rationally on priority.

The current state of research on Na−S and K−S batteries is at the laboratory level. Several practical issues need to be considered before its development and commercialization. As cost-effectiveness and energy density are essential indicators for commercial batteries, low-cost and large-scale production of catalytic materials are more desired, such as transition metals and their compounds. Considering the poor conductivity of most transition metal compounds, the design of catalytic materials needs to combine with the carbon material, which can also reduce the energy density of the battery. In addition, most catalytic materials are inactive in the redox reaction, leading to a further reduction in the energy density of the battery. For maximum utilization and maintaining an adequate proportion of catalytic materials in the electrode without compromising the energy density, identifying catalytic materials with high catalytic activity is critical. Further, it is also essential to explore and design novel catalytic materials and mechanisms to improve the electrochemical performances in Na−S and K−S batteries. Outcomes of such rational strategies can lead to extensive research prospects in metal-sulfur batteries and can be extended to other next-generation energy storage systems.

Credit author statement

A.K.H. conceptualization, investigation, validation, writing − original draft; C.H. conceptualization, validation, funding acquisition, writing − review & editing.

Declaration of competing interest

The authors declare that they have no known competing financial interests or personal relationships that could have appeared to influence the work reported in this paper.

Data availability

Data will be made available on request.

Acknowledgements

References

[1] H. Hesse, M. Schimpe, D. Kucevic, A. Jossen, Lithium-ion battery storage for the grid—a review of stationary battery storage system design tailored for applications in modern power grids, Energies 10 (2017).

[2] O. Schmidt, A. Hawkes, A. Gambhir, I. Staffell, The future cost of electrical energy storage based on experience rates, Nat. Energy 2 (2017).

[3] K. Kubota, M. Dahbi, T. Hosaka, S. Kumakura, S. Komaba, Towards K-ion and Na-ion batteries as "beyond Li-ion", Chem. Rec. 18 (2018) 459−479.

[4] S.H. Chung, A. Manthiram, Current status and future prospects of metal-sulfur batteries, Adv. Mater. 31 (2019), e1901125.

[5] Y.X. Wang, B. Zhang, W. Lai, Y. Xu, S.L. Chou, H.K. Liu, S.X. Dou, Room-temperature sodium-sulfur batteries: a comprehensive review on research progress and cell chemistry, Adv. Energy Mater. 7 (2017).

[6] J. Ding, H. Zhang, W. Fan, C. Zhong, W. Hu, D. Mitlin, Review of emerging potassium-sulfur batteries, Adv. Mater. 32 (2020), e1908007.

[7] N. Yabuuchi, K. Kubota, M. Dahbi, S. Komaba, Research development on sodium-ion batteries, Chem. Rev. 114 (2014) 11636−11682.

[8] H. Ye, Y. Li, Room-temperature metal−sulfur batteries: what can we learn from lithium−sulfur, InfoMat 4 (2022).

[9] I. Melián-Cabrera, Catalytic materials: concepts to understand the pathway to implementation, Ind. Eng. Chem. Res. 60 (2021) 18545−18559.

[10] A. Hu, C. Shu, C. Xu, R. Liang, J. Li, R. Zheng, M. Li, J. Long, Design strategies toward catalytic materials and cathode structures for emerging Li–CO$_2$ batteries, J. Mater. Chem. 7 (2019) 21605–21633.

[11] M.J. Muñoz-Batista, D. Rodriguez-Padron, A.R. Puente-Santiago, R. Luque, Mechanochemistry: toward sustainable design of advanced nanomaterials for electrochemical energy storage and catalytic applications, ACS Sustain. Chem. Eng. 6 (2018) 9530–9544.

[12] P. Wang, B. Xi, M. Huang, W. Chen, J. Feng, S. Xiong, Emerging catalysts to promote kinetics of lithium–sulfur batteries, Adv. Energy Mater. 11 (2021).

[13] H. Chen, Z. Wu, M. Zheng, T. Liu, C. Yan, J. Lu, S. Zhang, Catalytic materials for lithium-sulfur batteries: mechanisms, design strategies and future perspective, Mater. Today 52 (2022) 364–388.

[14] D. Liu, C. Zhang, G. Zhou, W. Lv, G. Ling, L. Zhi, Q.H. Yang, Catalytic effects in lithium-sulfur batteries: promoted sulfur transformation and reduced shuttle effect, Adv. Sci. 5 (2018), 1700270.

[15] Z. Yang, R. Xiao, X. Zhang, X. Wang, D. Zhang, Z. Sun, F. Li, Role of catalytic materials on conversion of sulfur species for room temperature sodium–sulfur battery, Energy & Environmental Materials 5 (2021) 693–710.

[16] C. Ye, J. Shan, D. Chao, P. Liang, Y. Jiao, J. Hao, Q. Gu, K. Davey, H. Wang, S.Z. Qiao, Catalytic oxidation of K2S via atomic Co and pyridinic N synergy in potassium-sulfur batteries, J. Am. Chem. Soc. 143 (2021) 16902–16907.

[17] L. Medenbach, P. Adelhelm, Cell concepts of metal-sulfur batteries (metal = Li, Na, K, Mg): strategies for using sulfur in energy storage applications, Top. Curr. Chem. 375 (2017) 81.

[18] F. Shi, J. Yu, C. Chen, S.P. Lau, W. Lv, Z.-L. Xu, Advances in understanding and regulation of sulfur conversion processes in metal–sulfur batteries, J. Mater. Chem. 10 (2022) 19412–19443.

[19] A.P. Vijaya Kumar Saroja, Y. Xu, Carbon materials for Na-S and K-S batteries, Matter 5 (2022) 808–836.

[20] A. Manthiram, X. Yu, Ambient temperature sodium-sulfur batteries, Small 11 (2015) 2108–2114.

[21] Y. Wang, D. Zhou, V. Palomares, D. Shanmukaraj, B. Sun, X. Tang, C. Wang, M. Armand, T. Rojo, G. Wang, Revitalising sodium–sulfur batteries for non-high-temperature operation: a crucial review, Energy Environ. Sci. 13 (2020) 3848–3879.

[22] X. Yu, A. Manthiram, Capacity enhancement and discharge mechanisms of room-temperature sodium-sulfur batteries, Chemelectrochem 1 (2014) 1275–1280.

[23] J. Sangster, A.D. Pelton, The Na-S (Sodium-Sulfur) system, J. Phase Equil. 18 (1997) 89–96.

[24] X. Yu, A. Manthiram, Electrochemical energy storage with a reversible nonaqueous room-temperature aluminum–sulfur chemistry, Adv. Energy Mater. 7 (2017).

[25] S. Xin, Y.X. Yin, Y.G. Guo, L.J. Wan, A high-energy room-temperature sodium-sulfur battery, Adv. Mater. 26 (2014) 1261–1265.

[26] X. Yu, A. Manthiram, A reversible nonaqueous room-temperature potassium-sulfur chemistry for electrochemical energy storage, Energy Storage Mater. 15 (2018) 368–373.

[27] P. Xiong, X. Han, X. Zhao, P. Bai, Y. Liu, J. Sun, Y. Xu, Room-temperature potassium-sulfur batteries enabled by microporous carbon stabilized small-molecule sulfur cathodes, ACS Nano 13 (2019) 2536–2543.

[28] W. Zhang, J. Yin, W. Wang, Z. Bayhan, H.N. Alshareef, Status of rechargeable potassium batteries, Nano Energy 83 (2021).

[29] J. Sangster, A.D. Pelton, The K-S (Potassium-Sulfur) system, J. Phase Equil. 18 (1997) 82–88.

[30] D.P. Shoemaker, D.Y. Chung, J.F. Mitchell, T.H. Bray, L. Soderholm, P.J. Chupas, M.G. Kanatzidis, Understanding fluxes as media for directed synthesis: in situ local structure of molten potassium polysulfides, J. Am. Chem. Soc. 134 (2012) 9456–9463.

[31] X. Yuan, B. Zhu, J. Feng, C. Wang, X. Cai, K. Qiao, R. Qin, Electrochemical insights, developing strategies, and perspectives toward advanced potassium-sulfur batteries, Small 16 (2020), e2003386.

[32] N.-C. Lai, G. Cong, Y.-C. Lu, A high-energy potassium–sulfur battery enabled by facile and effective imidazole-solvated copper catalysts, J. Mater. Chem. 7 (2019) 20584–20589.

[33] R. Ma, L. Fan, J. Wang, B. Lu, Confined and covalent sulfur for stable room temperature potassium-sulfur battery, Electrochim. Acta 293 (2019) 191–198.

[34] S. Gu, N. Xiao, F. Wu, Y. Bai, C. Wu, Y. Wu, Chemical synthesis of K2S2 and K2S3 for probing electrochemical mechanisms in K–S batteries, ACS Energy Lett. 3 (2018) 2858–2864.

[35] S. Zhang, Y. Yao, Y. Yu, Frontiers for room-temperature sodium–sulfur batteries, ACS Energy Lett. 6 (2021) 529–536.

[36] Z. Yan, Y. Liang, W. Hua, X.G. Zhang, W. Lai, Z. Hu, W. Wang, J. Peng, S. Indris, Y. Wang, S.L. Chou, H. Liu, S.X. Dou, Multiregion janus-featured cobalt phosphide-cobalt composite for highly reversible room-temperature sodium-sulfur batteries, ACS Nano 14 (2020) 10284–10293.

[37] X. Zhao, Y. Lu, Z. Qian, R. Wang, Z. Guo, Potassium-sulfur batteries: status and perspectives, EcoMat 2 (2020).

[38] I. Bauer, M. Kohl, H. Althues, S. Kaskel, Shuttle suppression in room temperature sodium-sulfur batteries using ion selective polymer membranes, Chem. Commun. 50 (2014) 3208–3210.

[39] D. Zhou, Y. Chen, B. Li, H. Fan, F. Cheng, D. Shanmukaraj, T. Rojo, M. Armand, G. Wang, A stable quasi-solid-state sodium-sulfur battery, Angew Chem. Int. Ed. Engl. 57 (2018) 10168–10172.

[40] Z. Li, Y. Sun, X. Wu, H. Yuan, Y. Yu, Y. Tan, Boosting adsorption and catalysis of polysulfides by multifunctional separator for lithium−sulfur batteries, ACS Energy Lett. (2022) 4190–4197.

[41] Q. Zhao, Y. Hu, K. Zhang, J. Chen, Potassium-sulfur batteries: a new member of room-temperature rechargeable metal-sulfur batteries, Inorg. Chem. 53 (2014) 9000–9005.

[42] L. Wang, J. Bao, Q. Liu, C.F. Sun, Concentrated electrolytes unlock the full energy potential of potassium-sulfur battery chemistry, Energy Storage Mater. 18 (2019) 470–475.

[43] L. Ren, Q. Wang, Y. Li, C. Hu, Y. Zhao, L. Qiao, H. Zhou, W. Liu, H. Xu, X. Sun, Catalytic separators with Co–N–C nanoreactors for high-performance lithium−sulfur batteries, Inorg. Chem. Front. 8 (2021) 3066–3076.

[44] Z. Du, X. Chen, W. Hu, C. Chuang, S. Xie, A. Hu, W. Yan, X. Kong, X. Wu, H. Ji, L.J. Wan, Cobalt in nitrogen-doped graphene as single-atom catalyst for high-sulfur content lithium-sulfur batteries, J. Am. Chem. Soc. 141 (2019) 3977–3985.

[45] B.W. Zhang, T. Sheng, Y.D. Liu, Y.X. Wang, L. Zhang, W.H. Lai, L. Wang, J. Yang, Q.F. Gu, S.L. Chou, H.K. Liu, S.X. Dou, Atomic cobalt as an efficient electro-catalyst in sulfur cathodes for superior room-temperature sodium-sulfur batteries, Nat. Commun. 9 (2018) 4082.

[46] X. Fan, S. Chen, W. Gong, X. Meng, Y. Jia, Y. Wang, S. Hong, L. Zheng, L. Zheng, C.W. Bielawski, J. Geng, A conjugated porous polymer complexed with a single-atom cobalt catalyst as an electrocatalytic sulfur host for enhancing cathode reaction kinetics, Energy Storage Mater. 41 (2021) 14–23.

[47] X. Liu, S. Wang, A. Wang, J. Chen, Z. Wang, Q. Zeng, W. Liu, Z. Li, L. Zhang, A new conjugated porous polymer with covalently linked polysulfide as cathode material for high-rate capacity and high coulombic efficiency lithium−sulfur batteries, J. Phys. Chem. C 123 (2019) 21327–21335.

[48] Y. Xiao, W. Gong, S. Guo, Y. Ouyang, D. Li, X. Li, Q. Zeng, W. He, H. Deng, C. Tan, Q. Zhang, S. Huang, Regulating coordination environment in metal−organic frameworks for adsorption and redox conversion of polysulfides in lithium−sulfur batteries, ACS Materials Letters 3 (2021) 1684–1694.

[49] D. Yang, Z. Liang, P. Tang, C. Zhang, M. Tang, Q. Li, J.J. Biendicho, J. Li, M. Heggen, R.E. Dunin-Borkowski, M. Xu, J. Llorca, J. Arbiol, J.R. Morante, S.L. Chou, A. Cabot, A high conductivity 1D pi-d conjugated metal-organic framework with efficient polysulfide trapping-diffusion-catalysis in lithium−sulfur batteries, Adv. Mater. 34 (2022), e2108835.

[50] M. Cheng, R. Yan, Z. Yang, X. Tao, T. Ma, S. Cao, F. Ran, S. Li, W. Yang, C. Cheng, Polysulfide catalytic materials for fast-kinetic metal-sulfur batteries: principles and active centers, Adv. Sci. 9 (2022), e2102217.

[51] Z. Yan, J. Xiao, W. Lai, L. Wang, F. Gebert, Y. Wang, Q. Gu, H. Liu, S.L. Chou, H. Liu, S.X. Dou, Nickel sulfide nanocrystals on nitrogen-doped porous carbon nanotubes with high-efficiency electrocatalysis for room-temperature sodium-sulfur batteries, Nat. Commun. 10 (2019) 4793.

[52] S. Luo, J. Ruan, Y. Wang, H.Y. Song, M. Chen, L. Wu, Flower-like interlayer-expanded MoS2-x nanosheets confined in hollow carbon spheres with high-efficiency electrocatalysis sites for advanced sodium-sulfur battery, Small 17 (2021), e2101879.

[53] B.S. Reddy, M. Premasudha, K.-M. oh, N.S. Reddy, H.-J. Ahn, J.-H. Ahn, K.-K. Cho, Hydrothermal synthesis of MoS2/rGO composite as sulfur hosts for room temperature sodium-sulfur batteries and its electrochemical properties, J. Energy Storage 39 (2021).

[54] B.-W. Zhang, S. Li, H.-L. Yang, X. Liang, W.-H. Lai, S. Zhao, J. Dong, S.-Q. Chu, Q.-F. Gu, J. Liang, Y. Du, X. Xu, L. Cao, Y.-X. Wang, F. Pan, S.-L. Chou, H.-K. Liu, S.-X. Dou, Atomically dispersed S-Fe-N4 for fast kinetics sodium-sulfur batteries via a dual function mechanism, Cell Reports Physical Science 2 (2021).

[55] Q. Ma, G. Du, B. Guo, W. Tang, Y. Li, M. Xu, C. Li, Carbon-wrapped cobalt nanoparticles on graphene aerogel for solid-state room-temperature sodium-sulfur batteries, Chem. Eng. J. 388 (2020).

[56] C. Ye, Y. Jiao, D. Chao, T. Ling, J. Shan, B. Zhang, Q. Gu, K. Davey, H. Wang, S.Z. Qiao, Electron-state confinement of polysulfides for highly stable sodium-sulfur batteries, Adv. Mater. 32 (2020), e1907557.

[57] X. Ge, H. Di, P. Wang, X. Miao, P. Zhang, H. Wang, J. Ma, L. Yin, Metal-organic framework-derived nitrogen-doped cobalt nanocluster inlaid porous carbon as high-efficiency catalyst for advanced potassium-sulfur batteries, ACS Nano 14 (2020) 16022–16035.

[58] X. Chen, L. Peng, L. Wang, J. Yang, Z. Hao, J. Xiang, K. Yuan, Y. Huang, B. Shan, L. Yuan, J. Xie, Ether-compatible sulfurized polyacrylonitrile cathode with excellent performance enabled by fast kinetics via selenium doping, Nat. Commun. 10 (2019) 1021.

[59] S. Li, Z. Han, W. Hu, L. Peng, J. Yang, L. Wang, Y. Zhang, B. Shan, J. Xie, Manipulating kinetics of sulfurized polyacrylonitrile with tellurium as eutectic accelerator to prevent polysulfide dissolution in lithium-sulfur battery under dissolution-deposition mechanism, Nano Energy 60 (2019) 153–161.

[60] S. Li, Z. Zeng, J. Yang, Z. Han, W. Hu, L. Wang, J. Ma, B. Shan, J. Xie, High performance room temperature sodium−sulfur battery by eutectic acceleration in tellurium-doped sulfurized polyacrylonitrile, ACS Appl. Energy Mater. 2 (2019) 2956–2964.

[61] L. Wang, X. Chen, S. Li, J. Yang, Y. Sun, L. Peng, B. Shan, J. Xie, Effect of eutectic accelerator in selenium-doped sulfurized polyacrylonitrile for high

performance room temperature sodium—sulfur batteries, J. Mater. Chem. 7 (2019) 12732—12739.

[62] S. Ma, P. Zuo, H. Zhang, Z. Yu, C. Cui, M. He, G. Yin, Iodine-doped sulfurized polyacrylonitrile with enhanced electrochemical performance for room-temperature sodium/potassium sulfur batteries, Chem. Commun. 55 (2019) 5267—5270.

[63] J. He, A. Manthiram, A review on the status and challenges of electrocatalysts in lithium-sulfur batteries, Energy Storage Mater. 20 (2019) 55—70.

[64] J. Zhang, C. You, H. Lin, J. Wang, Electrochemical Kinetic Modulators in Lithium—Sulfur Batteries: from Defect-Rich Catalysts to Single Atomic Catalysts, Energy & Environmental Materials, 2022.

[65] X. He, H. Hou, X. Yuan, L. Huang, J. Hu, B. Liu, J. Xu, J. Xie, J. Yang, S. Liang, X. Wu, Electrocatalytic activity of lithium polysulfides adsorbed into porous TiO$_2$ coated MWCNTs hybrid structure for lithium-sulfur batteries, Sci. Rep. 7 (2017), 40679.

[66] Q. Li, Z. Ma, J. Li, Z. Liu, L. Fan, X. Qin, G. Shao, Core-shell-structured sulfur cathode: ultrathin delta-MnO$_2$ nanosheets as the catalytic conversion shell for lithium polysulfides in high sulfur content lithium-sulfur batteries, ACS Appl. Mater. Interfaces 12 (2020) 35049—35057.

[67] P. Wang, R. Zeng, L. You, H. Tang, J. Zhong, S. Wang, T. Yang, J. Liu, Graphene-like matrix composites with Fe$_2$O$_3$ and Co$_3$O$_4$ as cathode materials for lithium—sulfur batteries, ACS Appl. Nano Mater. 3 (2020) 1382—1390.

[68] S. Wang, X. Hou, Z. Zhong, K. Shen, G. Zhang, L. Yao, F. Chen, Co$_3$O$_4$-NP embedded mesoporous carbon rod with enhanced electrocatalytic conversion in lithium-sulfur battery, Sci. Rep. 8 (2018), 16133.

[69] W. Du, Y. Wu, T. Yang, B. Guo, D. Liu, S.-J. Bao, M. Xu, Rational construction of rGO/VO2 nanoflowers as sulfur multifunctional hosts for room temperature Na-S batteries, Chem. Eng. J. 379 (2020).

[70] A. Kumar, A. Ghosh, A. Roy, M.R. Panda, M. Forsyth, D.R. MacFarlane, S. Mitra, High-energy density room temperature sodium-sulfur battery enabled by sodium polysulfide catholyte and carbon cloth current collector decorated with MnO$_2$ nanoarrays, Energy Storage Mater. 20 (2019) 196—202.

[71] A. Kumar, A. Ghosh, A. Ghosh, A. Ahuja, M. Forsyth, D.R. MacFarlane, S. Mitra, Approach to increase the utilization of active material in a high sulfur-loaded cathode for high areal capacity room-temperature sodium—sulfur batteries, ACS Appl. Energy Mater. 4 (2021) 384—393.

[72] A. Kumar, A. Ghosh, A. Ghosh, A. Ahuja, A. Sengupta, M. Forsyth, D.R. MacFarlane, S. Mitra, Sub-zero and room-temperature sodium—sulfur battery cell operations: a rational current collector, catalyst and sulphur-host design and study, Energy Storage Mater. 42 (2021) 608—617.

[73] E. Ceylan Cengiz, Z. Erdol, B. Sakar, A. Aslan, A. Ata, O. Ozturk, R. Demir-Cakan, Investigation of the effect of using Al2O3—nafion barrier on room-temperature Na—S batteries, J. Phys. Chem. C 121 (2017) 15120—15126.

[74] A.P. Vijaya Kumar Saroja, K. M, R. Sundara, Core—shell cathode design with molybdenum trioxide as the electrocatalytic trapping layer for high-energy density room-temperature sodium sulfur batteries, J. Phys. Chem. C 124 (2020) 7615—7623.

[75] R. Saroha, J. Heo, Y. Liu, N. Angulakshmi, Y. Lee, K.K. Cho, H.-J. Ahn, J.-H. Ahn, V$_2$O$_3$-decorated carbon nanofibers as a robust interlayer for long-lived, high-performance, room-temperature sodium—sulfur batteries, Chem. Eng. J. 431 (2022).

[76] X. Yuan, B. Zhu, J. Feng, C. Wang, X. Cai, R. Qin, An in-situ catalytic-insoluble strategy enabled by sulfurized polyacrylonitrile-based composite cathode for potassium—sulfur batteries, Funct. Mater. Lett. 14 (2021).

[77] J. Zhou, Y. Yang, Y. Zhang, S. Duan, X. Zhou, W. Sun, S. Xu, Sulfur in amorphous silica for an advanced room-temperature sodium-sulfur battery, Angew. Chem., Int. Ed. Engl. 60 (2021) 10129—10136.

[78] M. Zhang, W. Chen, L. Xue, Y. Jiao, T. Lei, J. Chu, J. Huang, C. Gong, C. Yan, Y. Yan, Y. Hu, X. Wang, J. Xiong, Adsorption-catalysis design in the lithium-sulfur battery, Adv. Energy Mater. 10 (2019).

[79] Y. Xiao, S.H. Lee, Y.-K. Sun, The application of metal sulfides in sodium ion batteries, Adv. Energy Mater. 7 (2017).

[80] X. Peng, Y. Yan, X. Jin, C. Huang, W. Jin, B. Gao, P.K. Chu, Recent advance and prospectives of electrocatalysts based on transition metal selenides for efficient water splitting, Nano Energy 78 (2020).

[81] W. Xiao, Q. He, Y. Zhao, Virtual screening of two-dimensional selenides and transition metal doped SnSe for lithium-sulfur batteries: a first-principles study, Appl. Surf. Sci. 570 (2021).

[82] C. Dong, H. Zhou, B. Jin, W. Gao, X. Lang, J. Li, Q. Jiang, Enabling high-performance room-temperature sodium/sulfur batteries with few-layer 2H-MoSe2 embellished nitrogen-doped hollow carbon spheres as polysulfide barriers, J. Mater. Chem. 9 (2021) 3451—3463.

[83] F. Xiao, H. Wang, T. Yao, X. Zhao, X. Yang, D.Y.W. Yu, A.L. Rogach, MOF-derived CoS2/N-doped carbon composite to induce short-chain sulfur

molecule generation for enhanced sodium-sulfur battery performance, ACS Appl. Mater. Interfaces 13 (2021) 18010—18020.

[84] H. Wang, C. Deng, X. Li, D. Yan, M. Xie, S. Zhang, B. Huang, Designing dual-defending system based on catalytic and kinetic iron Pyrite@C hybrid fibers for long-life room-temperature sodium-sulfur batteries, Chem. Eng. J. 420 (2021).

[85] S. Xin, L. Gu, N.H. Zhao, Y.X. Yin, L.J. Zhou, Y.G. Guo, L.J. Wan, Smaller sulfur molecules promise better lithium-sulfur batteries, J. Am. Chem. Soc. 134 (2012) 18510—18513.

[86] F. Xiao, H. Wang, J. Xu, W. Yang, X. Yang, D.Y.W. Yu, A.L. Rogach, Generating short-chain sulfur suitable for efficient sodium—sulfur batteries via atomic copper sites on a N,O-codoped carbon composite, Adv. Energy Mater. 11 (2021).

[87] Y. Zhang, Y. Guo, B. Wang, Y. Wei, P. Jing, H. Wu, Z. Dai, M. Wang, Y. Zhang, An integrated hybrid interlayer for polysulfides/selenides regulation toward advanced Li—SeS2 batteries, Carbon 161 (2020) 413—422.

[88] X. Li, J. Liang, J. Luo, C. Wang, X. Li, Q. Sun, R. Li, L. Zhang, R. Yang, S. Lu, H. Huang, X. Sun, High-performance Li-SeSx all-solid-state lithium batteries, Adv. Mater. 31 (2019), e1808100.

[89] W. Zhang, H. Wang, N. Zhang, H. Liu, Z. Chen, L. Zhang, S. Guo, D. Li, J. Xu, One-step in situ preparation of polymeric selenium sulfide composite as a cathode material for enhanced sodium/potassium storage, ACS Appl. Mater. Interfaces 11 (2019) 29807—29813.

[90] F. Zhou, Z. Li, X. Luo, T. Wu, B. Jiang, L.L. Lu, H.B. Yao, M. Antonietti, S.H. Yu, Low cost metal carbide nanocrystals as binding and electrocatalytic sites for high performance Li-S batteries, Nano Lett. 18 (2018) 1035—1043.

[91] G. Qin, Y. Liu, P. Han, S. Cao, X. Guo, Z. Guo, High performance room temperature Na-S batteries based on FCNT modified Co3C-Co nanocubes, Chem. Eng. J. 396 (2020).

[92] J. Xie, Y. Xie, Transition metal nitrides for electrocatalytic energy conversion: opportunities and challenges, Chemistry 22 (2016) 3588—3598.

[93] M. Nagai, Transition-metal nitrides for hydrotreating catalyst—synthesis, surface properties, and reactivities, Appl. Catal. Gen. 322 (2007) 178—190.

[94] Z. Chen, W. Lv, F. Kang, J. Li, Theoretical investigation of the electrochemical performance of transition metal nitrides for lithium—sulfur batteries, J. Phys. Chem. C 123 (2019) 25025—25030.

[95] C. Ye, H. Jin, J. Shan, Y. Jiao, H. Li, Q. Gu, K. Davey, H. Wang, S.Z. Qiao, A Mo5N6 electrocatalyst for efficient Na2S electrodeposition in room-temperature sodium-sulfur batteries, Nat. Commun. 12 (2021) 7195.

[96] A.P. Vijaya Kumar Saroja, A. Rajamani, K. Muthusamy, R. Sundara, Repelling polysulfides using white graphite introduced polymer membrane as a shielding layer in ambient temperature sodium sulfur battery, Adv. Mater. Interfac. 6 (2019).

[97] Z. Huang, B. Song, H. Zhang, F. Feng, W. Zhang, K. Lu, Q. Chen, High-capacity and stable sodium-sulfur battery enabled by confined electrocatalytic polysulfides full conversion, Adv. Funct. Mater. 31 (2021).

[98] X. Ye, J. Ruan, Y. Pang, J. Yang, Y. Liu, Y. Huang, S. Zheng, Enabling a stable room-temperature sodium-sulfur battery cathode by building heterostructures in multichannel carbon fibers, ACS Nano 15 (2021) 5639—5648.

[99] M. Naguib, M. Kurtoglu, V. Presser, J. Lu, J. Niu, M. Heon, L. Hultman, Y. Gogotsi, M.W. Barsoum, Two-dimensional nanocrystals produced by exfoliation of Ti3AlC2, Adv. Mater. 23 (2011) 4248—4253.

[100] M.R. Lukatskaya, S. Kota, Z. Lin, M.-Q. Zhao, N. Shpigel, M.D. Levi, J. Halim, P.-L. Taberna, M.W. Barsoum, P. Simon, Y. Gogotsi, Ultra-high-rate pseudocapacitive energy storage in two-dimensional transition metal carbides, Nat. Energy 2 (2017).

[101] J. Song, X. Guo, J. Zhang, Y. Chen, C. Zhang, L. Luo, F. Wang, G. Wang, Rational design of free-standing 3D porous MXene/rGO hybrid aerogels as polysulfide reservoirs for high-energy lithium—sulfur batteries, J. Mater. Chem. 7 (2019) 6507—6513.

[102] J. Zhang, Y. Zhao, X. Guo, C. Chen, C.-L. Dong, R.-S. Liu, C.-P. Han, Y. Li, Y. Gogotsi, G. Wang, Single platinum atoms immobilized on an MXene as an efficient catalyst for the hydrogen evolution reaction, Nature Catalysis 1 (2018) 985—992.

[103] X. Tang, D. Zhou, P. Li, X. Guo, B. Sun, H. Liu, K. Yan, Y. Gogotsi, G. Wang, MXene-based dendrite-free potassium metal batteries, Adv. Mater. 32 (2020), e1906739.

[104] W. Bao, C.E. Shuck, W. Zhang, X. Guo, Y. Gogotsi, G. Wang, Boosting performance of Na-S batteries using sulfur-doped Ti3C2Tx MXene nanosheets with a strong affinity to sodium polysulfides, ACS Nano 13 (2019) 11500—11509.

[105] W. Bao, R. Wang, C. Qian, Z. Zhang, R. Wu, Y. Zhang, F. Liu, J. Li, G. Wang, Porous heteroatom-doped Ti3C2Tx MXene microspheres enable strong adsorption of sodium polysulfides for long-life room-temperature sodium-sulfur batteries, ACS Nano 15 (2021) 16207—16217.